Using What Is Accessible to Measure That Which Is Not: Necessity of Model of System

Claudio Cobelli and Andrea Caumo

Understanding the in vivo functioning of endocrine-metabolic systems requires the quantitative knowledge of system parameters like production/utilization of substrales, secretion/degradation of homones, and substrate-hormone signaling. Unfortunately, these system parameters are not directly accessible and an indirect measurement approach is needed based on a model of the system. We review first the principals of the model of system methodology focusing on compartmental and input-output modeling. Then, the model of system methodology is applied to the measurement of nonaccessible parameters/variables of the glucose system like glucose fluxes, insulin fluxes, and glucose-insulin signaling.

UNDERSTANDING THE IN VIVO functioning of endocrine-metabolic systems at the whole-body or regional level requires the quantitative knowledge of system parameters like production/utilization of substrates, secretion/degradation of hormones, substrate/hormone masses in organ/tissues of the body, and substrate-to-hormone and hormone-to-substrate signaling. Unfortunately, these system parameters are not directly measurable, since the underlying events occur in the *nonaccessible* portion of the system (Fig 1). What can be measured is their effect in the *accessible* pool, usually plasma, where substrate/hormone concentrations can be monitored both in steady- and non–steady-state. Therefore, the measurement of the system parameters requires an *indirect* approach, ie, one has to link the accessible pool measurements with the nonaccessible system properties. This requires to make some assumptions on how the nonaccessible portion of the system works and to describe them mathematically, ie, to postulate a mathematical *model of system.* Mathematical models are not the only kind of models of real systems, eg, one also has verbal models, conceptual models, and physical models, but their power lies in their quantitative prediction nature. The model of system idea can be appreciated by looking at the example shown in Fig 2: if a model of system is postulated, one can use the accessible pool measurements to arrive at a numerical picture of the nonaccessible portion of the system, and thus at the desidered system parameters.

Two basic principles are usually combined for constructing a model, ie, structural modeling and parameter estimation (Fig 3). *Structural modeling* is essentially based on the collected experiences of the experts and the literature in the area of question and uses insight into the system structure combined with known physical laws to derive the mathematical model. However, at variance with technical systems, where the properties of the system can be broken down to subsystems whose behaviors are known and describable by the laws of nature, in nontechnical systems like a physiologic system, this is not possible, since the subsystem behavior is often not known and the well-known laws of nature are usually not available, even for simple subsystems. There is thus the need to introduce hypotheses or use generally recognized relationships. The other principle for model construction is *parameter estimation,* which exploits as the source of knowledge for the system properties the system itself. The idea is thus to use observations from the system to fit the model's properties to those of the system. This principle is normally used as a complement to structural modeling. In fact, in modeling a real system, neither of the two approaches is particularly fruitful in isolation and the two approaches must be combined. However, depending on the system and question being asked, one of the two modeling activities, ie, structural modeling or parameter estimation, may dominate the overall modeling effort.

Usually, there is a mismatch between the information content of the accessible pool measurements and the model of system necessary to estimate the desidered system parameters. *Dynamic data* are necessary and the tool of choice is the *tracer probe,* which is normally a radioactive or a stable isotope (Fig 4). Why do tracers help in augmenting the information content of the accessible pool measurements? Tracer data contain information on the system, since the tracer travels in the system like the original substance, the tracee, does (thanks to its indistinguishability and neglegible perturbation properties). In addition, they have a definite advantage with respect to tracee data: they need to be related to a simpler model of system, since the inputs of the tracer model are known, while those of the tracee model are not, since endogenous productions are present. Thus, one can resolve first the tracer model of the system (which reflects exchange and disposal processes only) and subsequently use it, in conjunction with the accessible pool tracee measurements, to arrive at the tracee model of the system. This applies both to the steady- and the non–steady-state. For instance, if glucose fluxes in the body need to be quantitated in the basal steady-state, one can obtain parameters like endogenous glucose production (equal to disposal, since the system is in steady-state), pool sizes, and fluxes in the body.[1,2] The non–steady-state situation is more difficult to tackle. For

From the Department of Electronics and Informatics, University of Padova, Padova, Italy; and San Raffaele Scientific Institute, Milano, Italy.

Submitted December 31, 1997; accepted December 31, 1997.

Based on a lecture given by one of the authors (C.C.) at the National Institutes of Health Symposium, "In Vivo Tracer Kinetics and Modeling," in honor of Dr Loren Zech, May 3, 1996, NIH, Bethesda, MD.

Supported in part by a grant from the Italian Ministero della Universita' e della Ricerca Scientifica e Tecnologica (Progetto 40%, Biosistemi e Bioinformatica) and by National Institutes of Health Grants No. RR02176 and RR 11095-02.

Address reprint requests to Professor Claudio Cobelli, Department of Electronics and Informatics, University of Padova, Via Gradenigo 6A, 35131 Padova, Italy.

0026-0495/98/4708-0021$03.00/0

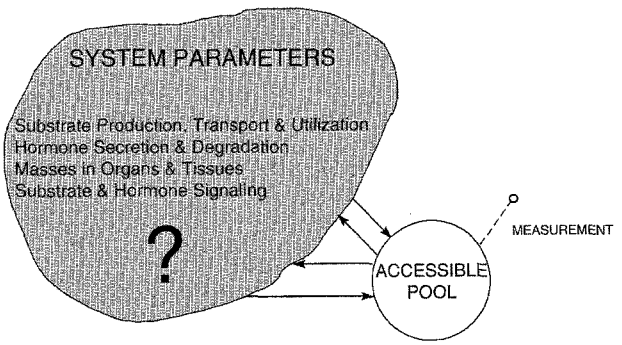

Fig 1. Schematic of an endocrine-metabolic system. System parameters are unknown and are not directly measurable. The accessible pool, ie, the only portion of the system accessible for measurement, is evidenced.

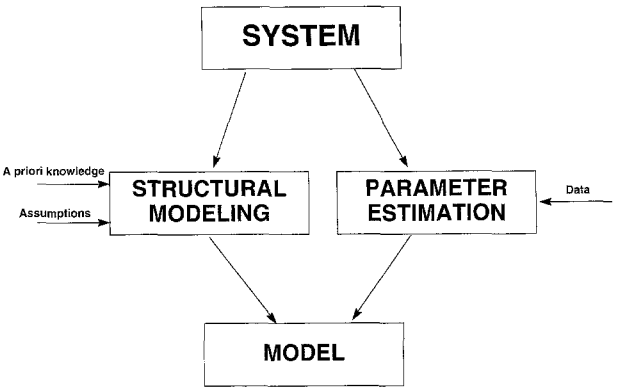

Fig 3. The ingredients of model construction.

instance, if one wants to quantitate endogenous glucose production and glucose disposal after a meal or a test like an oral glucose tolerance test (OGTT), there is the need to use two different glucose tracers, one given orally and one intravenously.[3] Another interesting example on how a tracer can increase the information content of a clinical test is provided by the intravenous glucose tolerance test (IVGTT). This test, when interpreted with the so-called minimal model of glucose kinetics,[4] is very informative and provides parameters like whole-body insulin sensitivity, ie, the effect of insulin in stimulating peripheral tissue glucose utilization and inhibiting its production, but it is not possible to separately describe the insulin effect on the liver and on the peripheral tissues. However, if a tracer is added to the glucose bolus and its time course is measured in plasma, a richer model of system can be resolved,[5-7] which allows segregation of the insulin effect on peripheral tissues from that on the liver.

At this point, it is clear that to quantitatively answer questions about the accessible and nonaccessible system properties from the accessible pool, we need a model of system and an adequate data base, ie, obtained by a suitably designed tracer experiment. In this report, we will concentrate on the model of system only, ie, we are not going to discuss issues related to tracer experiment design and measurement, like sites for tracer input and measurement,[8-10] how to express stable isotope measurements, and how to test for their possible perturbation.[11] The report is divided into two parts. The first part focuses on the model of system methodology and addresses issues like compartmental and input-output modeling, their numerical quantification from experimental data, and model validation. The second part illustrates the model of system methodology on a specific endocrine-metabolic system, the glucose-insulin system. It is worth remarking that the report is not a review of either the model of system methodology or of the glucose-insulin system. The spirit of the original lecture is maintained, ie, we will mostly use our own research results to illustrate how to attack the nonaccessible system parameter problem. While inevitably somewhat biased, we hope the report gives a flavor on how the model of system and tracer probe approach can be used to measure from what is accessible that which is not.

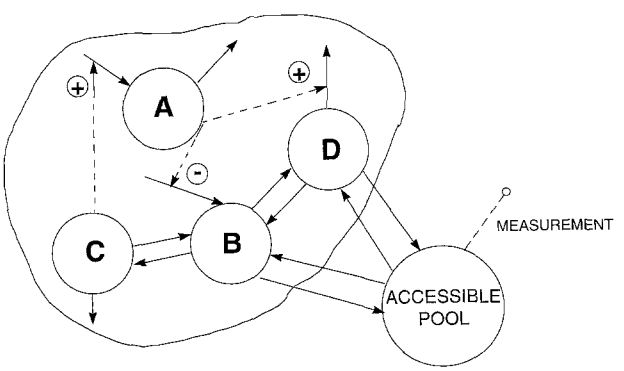

Fig 2. Example of a model of system. The nonaccessible portion of the system is modeled by a 4-pool structure. Continuous lines represent material fluxes and dashed lines control signals. In particular, A and B are de novo synthesized; A, C, and D utilized; A inhibits de novo synthesis of B and stimulates utilization of D; C stimulates de novo synthesis of A; C and D exchange with B; and B and D exchange with the accessible pool.

THE NONACCESSIBLE PARAMETERS PROBLEM: THE GLUCOSE SYSTEM PROTOTYPE

Before entering into the modeling methodology technicalities, it is worth particularizing the nonaccessible system parameter measurement problem for the glucose-insulin system, which will constitute our proof of the pudding. This system has been a major focus of our research interests in these last years. However, this system is also a good prototype, since all of the typical quantitative issues of a substrate-hormone system can be

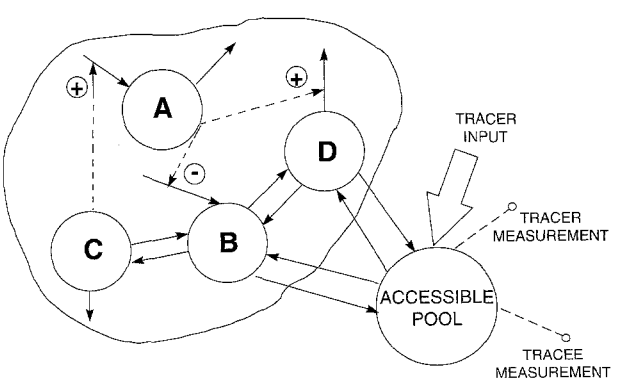

Fig 4. A tracer probe is used to augment the information content of the accessible pool measurements and estimate the unknown parameters of the model of system of Fig 2.

addressed. In addition, while showing many complexities, it is not too complex, eg, modeling amino acid and protein metabolism is much more challenging. A schematic representation of the system is shown in Fig 5. In the glucose subsystem, fluxes of glucose relate to endogenous glucose production and glucose utilization by tissues like the CNS, fat, and muscle. In the insulin subsystem, insulin fluxes represent insulin secretion by the pancreatic β cells, and insulin degradation by the liver, kidney, and peripheral tissues. The principal control signals allowing maintenance of glucose homeostasis are also shown, in particular glucose stimulation of β-cell secretion, insulin stimulatory effect on glucose utilization, and insulin inhibitory effect on endogenous glucose production. The goal is thus to quantify both glucose and insulin fluxes, as well as their signaling: these processes are not directly accessible to measurement and a model of system approach is needed.

COMPARTMENTAL MODELING

Models of system can have different characteristics depending on the properties of the system and the data base available for their study, ie, they can be deterministic or stochastic, dynamic or static, lumped or distributed parameter. Endocrine-metabolic systems are dynamic systems and we focus here on the most widely used class of dynamic (differential equation) models for their study, ie, compartmental models.[12,13] This is a class of models for which the governing law is conservation of mass and it is attractive to users, because it formalizes physical intuition in a simple and reasonable way. Compartmental models are lumped parameter models, ie, the events in the system are described by a finite number of changing variables, and are thus described by ordinary differential equations. We discuss here their deterministic version (stochastic compartmental models can also be defined), ie, those that work with exact relationships between model variables, which are by and large the most widely used in endocrinology and metabolism.

Compartmental models have been widely used for solving a broad spectrum of physiologic problems related to the distribution of materials in living systems in research, diagnosis, and therapy both at whole-body, organ, and cellular level. Examples and references can be found in several books and reviews.[12-21] The purposes for which compartmental models have been developed include the following: identification of system structure, ie, models to examine different hypotheses regarding the nature of specific physiologic mechanisms; estimation of unmeasurable quantities, ie, estimating internal parameters and variables of physiologic interest; simulation of the intact system behavior where ethical or technical reasons do not allow direct experimentation on the system itself; prediction and control of physiologic variables by administration of therapeutic agents, ie, models to predict an optimal administration of drug in order to keep one or more physiologic variables within desirable limits; optimizing cost effectiveness of dynamic clinical tests, ie, models to obtain maximal information from the minimum number of blood samples withdrawn from a patient; diagnosis, ie, models to augment quantitative information from laboratory tests and clinical symptoms, thus improving the reliability of diagnosis; and teaching, ie, models to aid in the teaching of many aspects of physiology, clinical medicine, and pharmacokinetics.

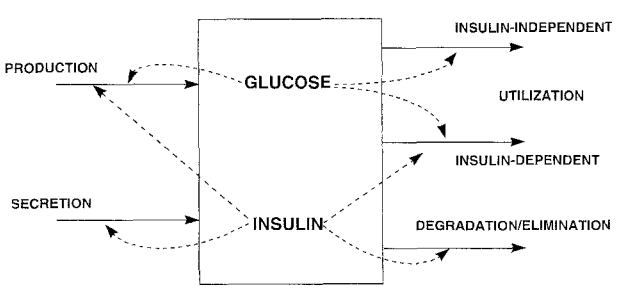

Fig 5. Schematic representation of the glucose-insulin system. Continuous lines represent fluxes of material; dashed lines represent control signals.

The use of compartmental models in physiology and pathophysiology has been made easier by the availability of the SAAM/CONSAM program,[22] a software specifically designed for compartmental models, which can be used both for simulation and fitting of models to data. Application of compartmental models is now even easier, since an entirely new version of SAAM, SAAM II,[23] has been developed. SAAM II retains the philosophy of the original version, but has a user-friendly graphical user interface, is fully menu-driven, and has an expanded and more sophisticated computational functionality. The formulation of compartmental model structures and the description of experimental protocols associated with models are therefore greatly facilitated.

Fundamentals

Before discussing the theory of compartmental models, we first need to give some definitions. A *compartment* is an amount of material that acts as though it is well mixed and kinetically homogeneous. A *compartmental model* consists of a finite number of compartments with specified interconnections among them. The interconnections represent a flux of material that physiologically represents transport from one location to another or a chemical transformation or both. An example is shown in Fig 6. Control signals arising in endocrine-metabolic control systems can also be described. In this case, one can have, for instance, two separate compartmental models, one for the hormone and one for the substrate, which interact via control signals. An example is shown in Fig 7.

Given the introductory definitions, it is useful before explaining well-mixed and kinetic homogeneity to consider possible candidates for compartments. Consider the notion of a compartment as a physical space. Plasma is a candidate for a compartment; a substance such as plasma glucose could be a compartment; zinc in bone could be a compartment also, as could insulin in β cells. In some experiments, different substances can be followed in plasma, eg, glucose, lactate, and alanine. Thus, in the same experiment, there can be more than one plasma compartment, one for each of the substances being studied. This notion extends beyond plasma. Glucose and glucose-6-phosphate can be two different compartments inside, eg, liver or muscle tissue. Thus, a physical space may actually represent more than one compartment.

In addition, one must distinguish between compartments that are accessible and nonaccessible for measurement. Researchers often try to assign physical spaces to the nonaccessible compartments. This is a difficult problem that is best addressed once one

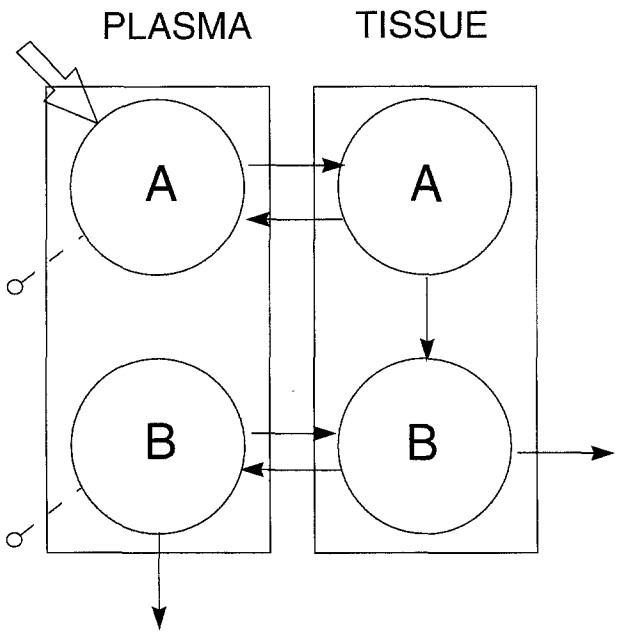

Fig 6. Example of a compartmental model. The administration of material into and sampling from the accessible pool are indicated by the input arrow and measurement symbols (dashed line with a bullet), respectively. Solid arrows represent the flux of material from one compartment to another.

realizes that the compartment is actually a theoretical construct, which may in fact lump material from several different physical spaces; to equate a compartment with a physical space depends on the system under study and assumptions about the model.

With these notions of what might constitute a compartment, it is easier to define the concepts of well-mixed and kinetic homogeneity. *Well-mixed* means that any two samples taken from the compartment at the same time would have the same concentration of the substance being studied and therefore be equally representative. Thus, the concept of well-mixed relates to uniformity of information contained in a single compartment.

Kinetic homogeneity means that every particle in a compartment has the same probability of taking the pathways that leave the compartment. Since, when a particle leaves a compartment, it does so because of metabolic events related to transport and utilization, it means that all particles in the compartment have the same probability of leaving due to one of these events.

The notion of a compartment, ie, lumping material with similar characteristics into collections that are homogeneous and behave identically, is what allows one to reduce a complex physiologic system into a finite number of compartments and pathways. The number of compartments required depends both on the system being studied and on the richness of the experimental configuration. A compartmental model is clearly unique for each system studied, since it incorporates known and hypothesized physiology and biochemistry. It provides the investigator with insights into the system structure and is as good as the assumptions that are incorporated in the model structure.

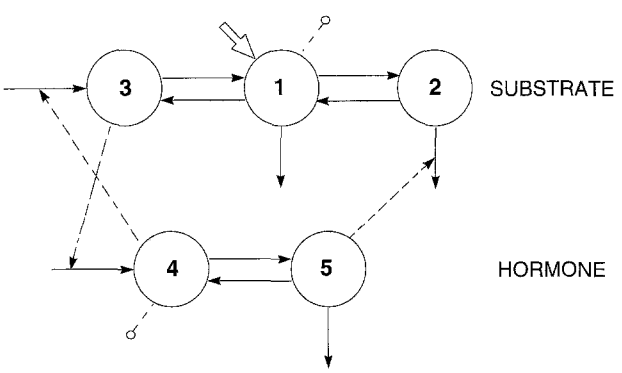

Fig 7. Example of a multicompartmental model of an endocrine-metabolic control system. The top and bottom multicompartmental models describe the metabolism of the substrate and hormone, respectively. Dashed lines represent control signals (examples are given in equations 8, 10, and 11). For example, the dashed line from compartment 3 to the input arrow into compartment 4 indicates that the amount of material in compartment 3 controls the input of material into compartment 4.

The Tracee Model

In this section, we will formalize the tracee model using Fig 8. This is a typical compartment, the i^{th} compartment. There is the need to define precisely the flux of tracee material into and out from this compartment, and the measurement equation if this compartment is accessible for sampling. Once this is understood, the notion of connecting several such compartments together into a multicompartmental model and writing the corresponding equations is easy.

Let Fig 8 represent the i^{th} compartment of an n-compartment model of the tracee system, with Q_i denoting the mass of the compartment. The arrows represent fluxes into and out of the compartment; the input flux into the compartment from outside the system, ie, de novo synthesis of material, is represented by F_{i0}; the flux to the environment and therefore out of the system by F_{0i}; the flux from compartment j to i by F_{ij}; finally U_h ($h = 1, \ldots, r$) denotes an exogenous input. All fluxes F_{ij} ($i = 0, 1, \ldots, n; j = 0, 1, \ldots, n; i \neq j$) and masses Q_i ($i = 1, 2, \ldots, n$) are ≥ 0. The dashed arrow with a bullet indicates that the compartment is accessible to measurement: the measurement is

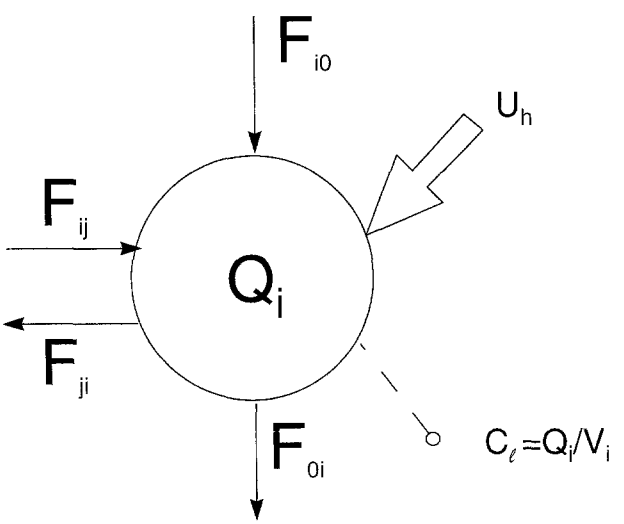

Fig 8. The i^{th} compartment of an n-compartment model showing fluxes into and out from the compartment, inputs, and measurements.

denoted by C_l ($l = 1, \ldots, m$), and we assume it is a concentration, ie, $C_l = Q_i/V_i$, where V_i is the volume of compartment i. As already noted, usually only a small number of compartments are accessible to test inputs and measurements.

By using the mass balance principle one can write for each compartment:

$$\begin{aligned}\dot{Q}_i(t) = &-\sum_{\substack{j=1\\ j\neq 1}}^{n} F_{ji}[Q_1(t), \ldots, Q_n(t)] - F_{0i}[Q_1(t), \ldots, Q_n(t)] \\ &+ \sum_{\substack{j=1\\ j\neq 1}}^{n} F_{ij}[Q_1(t), \ldots, Q_n(t)] \\ &+ F_{i0}[Q_1(t), \ldots, Q_n(t)] + U_h(t), \quad Q_i(0) = Q_{i0} \\ C_l(t) = &\, Q_i(t)/V_i\end{aligned} \tag{1}$$

where $\dot{Q}_i = (dQ_i/dt)$ and $t > 0$ is time, the independent variable. All the fluxes, F_{ij}, F_{i0}, and F_{0i}, are assumed to be functions of the compartmental masses Q_i ($i = 1, \ldots, n$).

If one writes the generic flux F_{ji} ($j = 0, 1, \ldots, n$; $i = 1, 2 \ldots n$; $j \neq i$) as

$$F_{ji}[Q_1(t), \ldots, Q_n(t)] = k_{ji}[Q_1(t), \ldots, Q_n(t)]Q_i(t) \tag{2}$$

where $k_{ji}(\geq 0)$ denotes the fractional transfer coefficient between compartment i and i, equation 1 can be written as:

$$\begin{aligned}\dot{Q}_i(t) = &-\sum_{\substack{j=0\\ j\neq i}}^{n} k_{ji}[Q_1(t), \ldots, Q_n(t)]Q_i(t) \\ &+ \sum_{\substack{j=0\\ j\neq i}}^{n} k_{ij}[Q_1(t), \ldots, Q_n(t)]Q_i \\ &+ F_{i0}[Q_1(t), \ldots, Q_n(t)] + U_h(t), \quad Q_i(0) = Q_{i0} \\ C_l(t) = &\, Q_i(t)/V_i\end{aligned} \tag{3}$$

Equation 3 describes the *nonlinear* compartmental model of the tracee system.

To make the model operative, one has to specify how the k_{ij} and F_{i0} depend on the Q_i. This obviously depends on the system being studied. Usually, k_{ij} and F_{i0} are functions of only a few of the Q_i. Possible examples are as follows:

- k_{ij} constant, ie, not dependent on any Q_i:

$$k_{ij}[Q_1(t), \ldots, Q_n(t)] = k_{ij} \tag{4}$$

- k_{ij} described by saturative relationship on the source compartment Q_j, eg, Michaelis-Menten:

$$k_{ij}[Q_j(t)] = \frac{V_M}{K_m + Q_j(t)} \tag{5}$$

or the Hill equation:

$$k_{ij}[Q_j(t)] = \frac{V_M Q_j^{q-1}(t)}{K_m Q_j^q(t)} \tag{6}$$

Note that when $q = 1$, equation 6 becomes equation 5.

- k_{ij} controlled by the arrival compartment Q_i, eg, by the Langmuir relationship:

$$k_{ij}[Q_i(t)] = \alpha\left\{1 - \frac{Q_i(t)}{\beta}\right\}. \tag{7}$$

- k_{ij} controlled by a remote compartment different from the source (Q_j) or arrival (Q_i) ones, eg, for the model shown in Fig 6, one could have:

$$k_{02}[Q_5(t)] = \gamma + Q_5(t) \tag{8}$$

or a more complex description as:

$$k_{02}[Q_2(t), Q_5(t)] = \frac{V_M[Q_5(t)]}{K_m[Q_5(t)] + Q_2(t)} \tag{9}$$

where now one has to further specify how V_M and K_m depend on the controlling compartment, Q_5.

- F_{i0} controlled by remote compartments, eg, for the model shown in Fig 6, one can have:

$$F_{30}[Q_4(t)] = \frac{\delta}{\epsilon + Q_4(t)} \tag{10}$$

$$F_{40}[Q_3(t)] = \eta + \lambda Q_3(t) + \mu\dot{Q}_3(t) \tag{11}$$

The nonlinear compartmental model given in equation 3 allows the description of an endocrine-metabolic system in non–steady-state under very general circumstances.

Having specified the number of compartments and the functional dependencies, there is now the problem of assigning a numerical value to the unknown parameters describing them. Some of them may be assumed to be known, but some need to be tuned to the particular system studied. In terms of the model construction scheme of Fig 4, up to here we have used the structural modeling principle and it is now time to turn to the parameter estimation principle, ie, one has to use the observations on the system to fit the model properties to those of the system. Often, however, the data are not enough to arrive at the unknown parameters of the model, and a tracer is usually employed to enhance the information content of the data.

The Tracer Model

In this section, we will formalize the definition of the tracer model using Fig 9. This parallels exactly the notions introduced earlier, except now we follow the tracer, denoted by lowercase letters, instead of the tracee. The link between the two, the tracee and the tracer models, is given in the following section.

Suppose an isotopic (radioactive or stable) tracer is injected (denoted by u_h) into the i^{th} compartment and denote $q_i(t)$ its tracer mass at time t (Fig 9). Assuming an ideal tracer, the tracer-tracee indistinguishability ensures that the tracee k_{ij} also apply to the tracer. Measurement is usually a concentration, for a radioactive tracer, ie, $y_l = q_i/V_i$, and the tracer-to-tracee ratio, ie, $y_l = q_i/Q_i$, for a stable isotope tracer.

The tracer model, given the tracee model of equation 3, is described by:

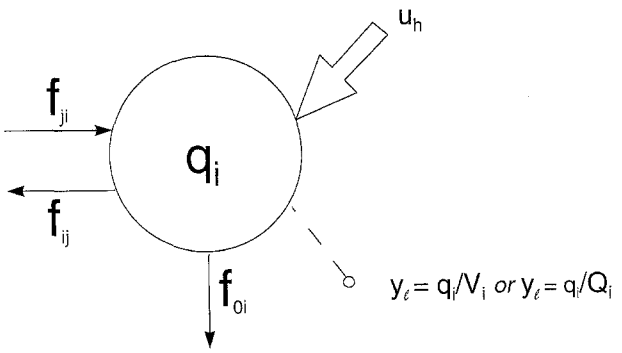

Fig 9. The i^{th} compartment of an n-compartment tracer model showing fluxes into and out from the compartment, inputs, and measurements.

$$\dot{q}_i(t) = -\sum_{\substack{j=0 \\ j\neq i}}^{n} k_{ji}[Q_1(t), \ldots, Q_n(t)]q_i(t) + \sum_{\substack{j=0 \\ j\neq i}}^{n} k_{ij}[Q_1(t), \ldots, Q_n(t)]q_j(t) + u_1(t), \quad q_i(0) = 0$$
$$y_1(t) = q_i(t)/V_i \text{ or } y_1(t) = q_i(t)/Q_i(t) \tag{12}$$

Note that the production terms F_{i0} of the tracee model (equation 3) does not appear in equation 12; this is because this term applies only to the tracee.

The Tracer-Tracee Model

The model of system necessary to arrive at the nonaccessible system properties is obtained by linking the tracee and tracer models to form the tracer-tracee model; this model is described by equations 3 and 12. The problem one wishes to solve is to use the tracee data C_1 and the tracer data y_1 to obtain the unknown parameters of the model. This is accomplished by using the parameter estimation principle described below.

Before going into the details of this problem, it is useful to consider an important special situation, the tracee steady-state case.

The tracee steady-state. If the tracee is in a constant steady-state, the exogenous input U_h is zero, all the fluxes F_{ij} and masses Q_i in the tracee model (equation 1) are constant, and the derivatives $\dot{Q}_i(t)$ are zero. As a result, all of the fractional transfer coefficients k_{ij} (see equation 2) are constant.

The tracee and tracer model given in equations 3 and 12, respectively, thus become:

$$0 = -\sum_{\substack{j=0 \\ j\neq i}}^{n} k_{ji}Q_i + \sum_{\substack{j=1 \\ j\neq i}}^{n} k_{ij}Q_j + F_{i0} \quad Q_i(0) = Q_{i0}.$$
$$C_1 = Q_i/V_i \tag{13}$$

$$\dot{q}_i(t) = -\sum_{\substack{j=0 \\ j\neq i}}^{n} k_{ji}q_i(t) + \sum_{\substack{j=1 \\ j\neq i}}^{n} k_{ij}q_j(t) + u_h(t) \quad q_i(0) = 0$$
$$y_1(t) = q_i(t)/V_i \text{ or } q_i(t)/Q_i \tag{14}$$

This is an important result: the tracer compartmental model is *linear* if the tracee is in a constant steady, irrespective of whether it is linear or nonlinear. The modeling machinery for equations 13 and 14 is greatly simplified with respect to the nonlinear model given in equations 3 and 12. The strategy is to use the tracer data to arrive at the k_{ij} and the accessible pool volume V_i or mass Q_i of equation 14, and subsequently use the steady-state tracee model of equation 13 to solve for the unknown parameters F_{i0} and the remaining Q_i. Note that from the k_{ij} parameter matrix, K, which can be defined from equation 14, one can calculate the mean residence time matrix Θ, as[12,13]:

$$\Theta = -K^{-1} \tag{15}$$

where θ_{ij} denotes the average time that a particle introduced into j will spend in compartment i before leaving it irreversibly. From Θ, some important parameters can be calculated, eg, the mean residence time a particle introduced into j will spend in the system before leaving it irreversibly, MRT^j, which is simply the sum of the elements of the j^{th} column of Θ.

As one can expect, there is a price to be paid for this simpler modeling machinery: one obtains a mechanistic picture of the steady-state operating point, but cannot describe the tracee system in its full nonlinear operation arising, for example, from saturation kinetics and control signals. To make this point clear, it is worth considering the simple example shown in Fig 10. The tracee system is in steady-state, but it is nonlinear: both its production and utilization are nonlinearly controlled by Q_1. The information an ideal, eg, stable isotope, tracer experiment can provide are parameters k_{01} (a constant) and Q_1 and thus utilization and production $F_{01} = k_{01}Q_1 = F_{10}$, but one cannot arrive at α, β, V_M, and K_m. This example was deliberately chosen as a simple one, but one can readily extend the reasoning

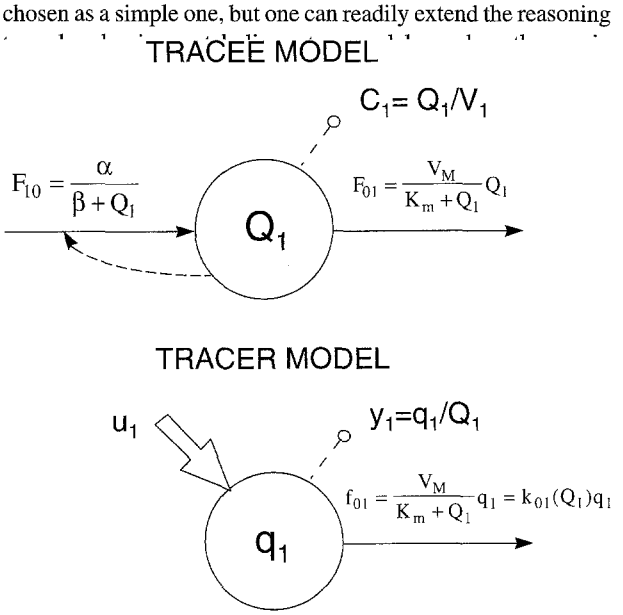

Fig 10. Example of a system where the tracee is in steady-state, but nonlinear.

use the more demanding nonsteady models of equations 3 and 12 discussed previously. An appealing alternative is to use multiple steady-state tracer modeling, ie, repeat the tracer experiment in various steady-states and use linear tracer modeling to describe the system in each of them. In this way, the information increases, eg, the k_{ij} for each of the various steady-states become available, and one can arrive at the parameters describing the functional dependencies of the tracee model.

It is worth mentioning that for the tracee steady-state case, another modeling approach, the so-called noncompartmental model, is available for interpreting the tracer data.[24-26] The one– and two–accessible pool noncompartmental models are shown in Fig 11A and B, respectively. Let us consider the one–accessible pool model (Fig 11A); it allows the substance to enter de novo into the accessible pool, to leave it irreversibly, and to distribute through an undetermined number of body compartments connected in whatever way (the curved arrow, which accounts for the nonaccessible portion of the system). From the model, some macroscopic system parameters can be estimated, like de novo production, mean residence time in the system of a particle introduced into the accessible pool, and total body mass. However, the model only provides lower bound estimates of these parameters, which coincide with those recovered by a compartmental model if and only if all de novo productions and irreversible losses of the system occur in the accessible pool. This applies to both the one– and the two–accessible pool noncompartmental model. Thus, the noncompartmental model provides some macroscopic parameters that are equivalent to those provided by a multicompartmental model with de novo productions and irreversible losses in the accessible pool only. The noncompartmental model, if the assumptions on its validity are satisfied and a macroscopic picture of the system is the target, is computationally less demanding than the compartmental model, since it essentially involves areas and the first moment of the area under the tracer concentration curve. Since theory predicts that tracer concentration is described by a sum of exponentials (see equation 26), one can use the nonlinear least-squares parameter estimation machinery described later to perform the required calculations.

The Measurement Equations

With the tracer-tracee model described by equations 3 and 12 (or equations 13 and 14 in steady-state conditions), we can now proceed to parameter estimation, ie, arrive at a numerical value of the unknown model parameters from the measurements. The measurement configuration for the tracee and tracer models has been described through the variables C_l and y_l in equations 3 and 12, respectively (or equations 13 and 14). However, real data are noisy, ie, they are affected by errors, and are usually collected at discrete time instants $t_1, \ldots, t_N$. Here, we will assume that measurement error is additive and the tracee and tracer actual measurements are thus described respectively by:

$$C_l^{obs}(t_i) = C_l(t_i) + E_l(t_i) \tag{16}$$

$$y_l^{obs}(t_i) = y_l(t_i) + e_l(t_i) \tag{17}$$

where E_l and e_l, are the measurement errors of tracee and tracer, respectively. The errors are usually given a probabilistic description, eg, they are assumed to be independent and often gaussian. With equations 16 and 17, and equations 3 and 12 (or equations 13 and 14), the compartmental parameter estimation problem can now be defined; specifically, it is estimating the unknown model parameters from the noisy data C_l^{obs} and y_l^{obs}.

Before solving this problem, we need to deal with a prerequisite issue for well-posedness of parameter estimation. This is a priori identifiability and, as seen later, this requires reasoning using ideal noise-free data, ie, equations 3 and 12 (or equations 13 and 14).

A Priori Identifiability

The following question arises before performing the experiment to collect the data to be analyzed using the model or, if the experiment is already completed, before using the model to estimate the unknown parameters from the data: do the data contain enough information to estimate all of the unknown parameters of the postulated model structure? This question is usually referred to as the *a priori identifiability* problem. It is set in the ideal context of error-free model structure and noise-free measurements (a priori), and is an obvious prerequisite to determine if parameter estimation from real data is well posed. In particular, if it turns out in such an ideal context that the postulated model structure is too complex for the particular set of ideal data, ie, some model parameters are not identifiable from the data, there is no way in a real situation—where there is error in the model structure and noise in the data—that the parameters can be identified. A priori identifiability is also crucial in experiment design,[8] which investigates the input-

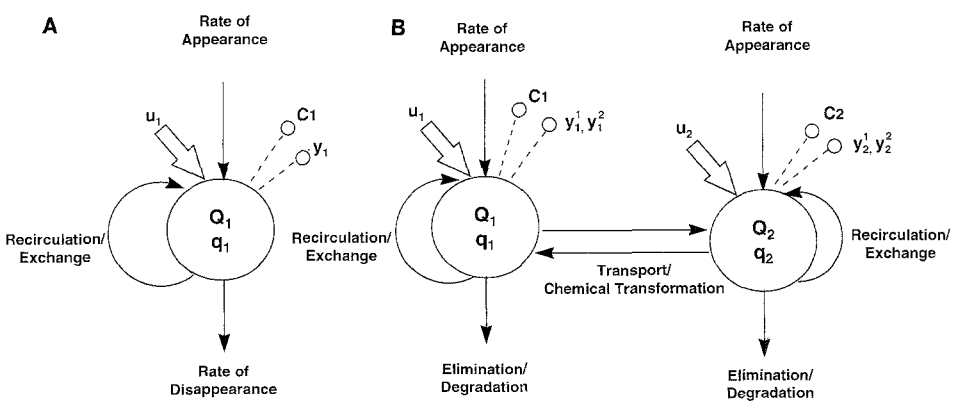

Fig 11. The 1– (A) and 2–accessible pool (B) noncompartmental model. In the 2–accessible pool model, it is assumed that 2 different tracers are administered simultaneously with y_1^1, y_1^2 denoting the tracer measurements in pool 1 and 2 due to tracer input u_1 and u_2, respectively, and y_2^1, y_2^2 denoting the tracer measurements in pool 2 due to tracer input u_1 and u_2, respectively.

output configuration necessary to ensure estimation of the unknown parameters. In particular, questions like which is the minimal input-output configuration can thus be answered.[9]

A priori identifiability thus examines whether, given the ideal noise-free data, and the error-free compartmental model structure of equations 3 and 12 (or equations 13 and 14), it is possible to make unique estimates of all the unknown model parameters. A model can be uniquely identifiable or nonuniquely identifiable—that is, one or more of the parameters has more than one but a finite number of possible values—or nonidentifiable—that is, one or more of the parameters has an infinite number of solutions.

A simple example on a linear two-compartment tracer model (Fig 12) can serve to better focus the problem. The model on the top is a priori uniquely identifiable from the ideal data y_1,[12,13] ie, V_1, k_{21}, k_{01}, and k_{21} can be uniquely estimated, while the bottom model is nonidentifiable,[12,13] ie, V_1 can be uniquely estimated, but k_{21}, k_{01}, k_{12}, and k_{02} have an infinite number of solutions. This simply means that one pretends too much from the data, ie, the model is too complex for the designed experiment. Clearly, in no way can the actual measurements y_1^{obs}, ie, affected by errors and finite in number, improve the identifiability properties of this model. Knowing in advance the identifiability properties of a model is thus an obvious prerequisite.

The identifiability problem is, in general, a large nonlinear algebraic one and thus difficult to solve, since there is the need

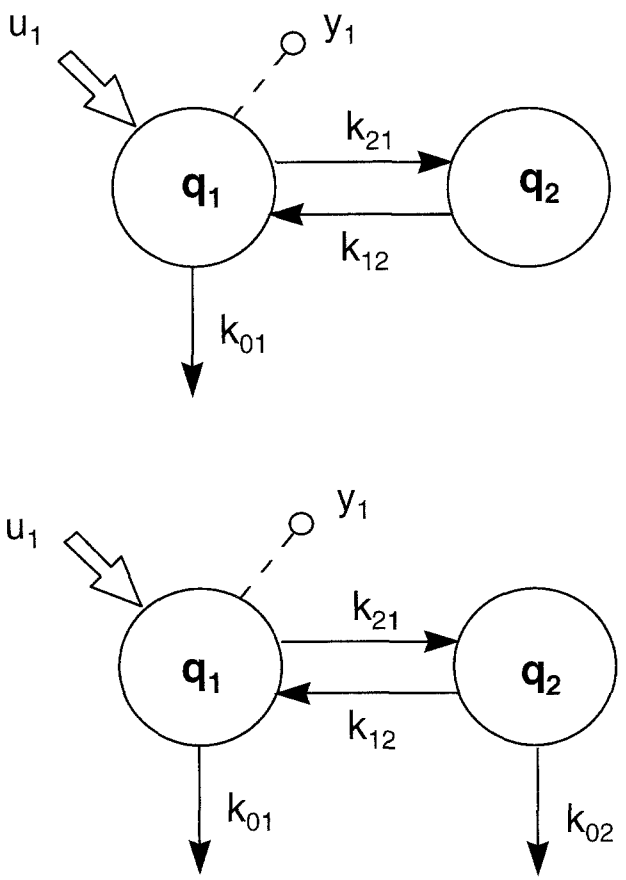

Fig 12. Two different compartment models. The upper model is uniquely identifiable, while the model shown below is not.

to solve a system of nonlinear algebraic equations that is increasing in number of terms and nonlinearity degree with the model order, ie, the number of compartments in the model. Various methods for testing identifiability of linear and nonlinear compartmental models are available.[12,13,27,28] For linear compartmental models, various specific methods based, eg, on the transfer function, have been developed. Explicit identifiability results on catenary and mamillary compartmental models[29] and on the two[13] and three-compartmental model[30] are also available. A parameter-bound strategy for dealing with nonidentifiable compartmental models has also been developed.[31] For nonlinear compartmental models, the problem is more difficult, and for small models, the output series expansion method[32] is usually employed.

However, all of the proposed methods apply to models of relatively low dimension; when applied to large models, the methods involve nonlinear algebraic equations too difficult to be solved even by resorting to symbolic algebraic manipulative languages (eg, Reduce, Maple). These difficulties have stimulated new approaches to study global identifiability based on computer algebra. In particular, for nonlinear models, approaches based on differential algebra have been investigated,[33,34] while for linear compartmental models, a method based on the transfer function and Gröbner basis algorithm has been proposed.[35]

If a model is a priori uniquely or nonuniquely identifiable, then parameter estimation techniques (eg, least squares) can be used to estimate from the noisy data, the numerical values of the unknown parameters. If a model is a priori nonidentifiable, then not all of its parameters can be estimated using parameter estimation techniques. Various strategies can be used, eg, derivation of bounds for nonidentifiable parameters, model reparameterization (parameter aggregation), incorporation of additional knowledge, or design of a more informative experiment. For an example on the use of these approaches for dealing with a nonidentifiable model of glucose kinetics we refer to Cobelli and Toffolo.[36]

From the above considerations, it follows that a priori unique identifiability is a prerequisite for well posedness of parameter estimation and for reconstructability of state variables in nonaccessible compartments. It is a necessary step, but, because of the ideal context where it is posed, it does not guarantee a successful estimation of model parameters from real input-output data.

Parameter Estimation and a Posteriori Identifiability

The parameter estimation problem deals with estimating the values of the unknown parameters of the model (equations 3 and 12, or equations 13 and 14) from the set of noisy real data described in equations 16 and 17. Below, we will discuss some underlying principals.

Basically, one needs a method that provides a set of numerical estimates of the parameters which best fit the data and a measure of their precision. The parameter estimation problem for both linear and nonlinear compartmental models is nonlinear (ie, parameters do not appear in the model linearly, like in a straight line or a polynomial model) and this makes it a difficult problem to handle (for details on parameter estimation of physiologic system models, we have to refer elsewhere[12,37]).

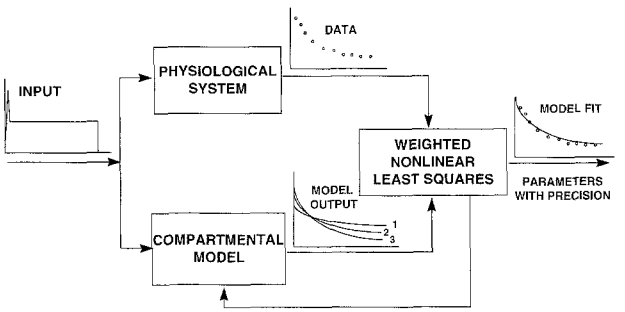

Fig 13. Schematic of WRSS minimization. The idea is to use iterated weighted nonlinear least squares to obtain a best fit to the data. At each iteraction step, a model output is generated, as indicated in the figure, and compared with the data. Model outputs 1, 2, and 3 could be the results of 3 successive iterations.

Weighted nonlinear least squares is the most commonly used parameter estimation technique. To better grasp the method, consider the linear compartmental model of equations 13 and 14 and suppose we want to estimate its parameters form a set of radioactive noisy data (equation 17). Weighted nonlinear least squares defines the weighted residual sum of squares (WRSS) as cost function:

$$\text{WRSS} = \sum_{i=1}^{N} \frac{1}{w_1(t_i)} [y_1^{obs}(t_i) - y_1(t_i; k_{ij}, V_1)]^2 \qquad (18)$$

and the parameter estimates $\hat{k}_{ij}$ and $\hat{V}_1$ are those which minimize WRSS.

As already pointed out, the model is nonlinear in the parameters, and thus there is no closed-form analytical solution to WRSS minimization as in the case of linear parameter problems (ie, linear regression for estimating straight line or polynomial parameters). This requires an iterative solution to WRSS minimization. Iteration can be thought of a series of steps where the nonlinear problem is handled in a linear fashion at each step in such a way that WRSS is minimized in moving from one step to the next. The interested reader can refer to Carson et al[12] for more details. This is illustrated schematically in Fig 13. Various robust techniques are available, eg, those based on successive linearizations of the model, so that at each iteration a linear least-squares problem needs to be solved. It is also clear that to start the iterative scheme with the model linearization, one needs an initial value for the unknown parameters and this adds to the difficulties of the problem.

Another important but critical ingredient of weighted nonlinear least squares is the choice of the weights [eg, the $w_1(t_i)$ in equation 18]. In fact, in order to have a correct summary of the statistical properties of the estimates, the weights should be chosen optimally,[12,37] ie, equal to the inverse of measurement error variances, $\sigma_1^2(t_i)$, if they are known, ie, $w_1(t_i) = 1/\sigma_1^2(t_i)$, or of their relative values if variances are known up to a proportionality constant, ie, if $\sigma_1^2(t_i) = v_1(t_i)\sigma^2$ with $v_1(t_i)$ known and σ^2 unknown, $w_1(t_i) = 1/v_1(t_i)$. Under these circumstances, one can obtain an approximation of the covariance matrix of the parameter estimates, which can be used to evaluate their precision, ie, their *a posteriori* or *numerical identifiability*. If we denote with **p** (dimension P) the vector of unknown parameters, the covariance matrix of parameter estimate) is given by:

$$\text{Cov}(\hat{\mathbf{p}}) = \begin{bmatrix} \text{Var}(\hat{p}_1) & \text{Cov}(\hat{p}_1, \hat{p}_2) & \cdots & \text{Cov}(\hat{p}_1, \hat{p}_P) \\ \text{Cov}(\hat{p}_2, \hat{p}_1) & \text{Var}(\hat{p}_2) & \cdots & \text{Cov}(\hat{p}_2, \hat{p}_P) \\ \vdots & & \ddots & \vdots \\ \text{Cov}(\hat{p}_P, \hat{p}_1) & \text{Cov}(\hat{p}_P, \hat{p}_2) & \cdots & \text{Var}(\hat{p}_P) \end{bmatrix} \qquad (19)$$

The diagonal of the covariance matrix contains the variances of the parameter estimates, and precision is usually expressed in terms of percent fractional standard deviation or coefficient of variation. For instance, if $\hat{k}_{ij}$ denotes the estimate of k_{ij} one calculates the percent fractional standard deviation or coefficient of variation as $CV(\hat{k}_{ij}) = 100\sqrt{\text{var}(\hat{k}_{ij})}/\hat{k}_{ij} = 100\,SD(\hat{k}_{ij})/\hat{k}_{ij}$.

A scheme that summarizes the various ingredients of weighted nonlinear least squares from the user's point of view is shown in Fig 14. One has obviously to supply the data and the model, but also the measurement error of the data, which will be used to assign the weights and an initial estimate for each of the unknown parameters. From weighted nonlinear least squares, one obtains the model fit to the data and has the residuals (the difference between the datum and the model predicted value at specific sample time), the estimated parameter values, and their precision.

The quantitative assessment of model quality from parameter estimation is crucial, as it is also an essential component of model validation. One has first to examine the quality of model predictions to observed data. In addition to visual inspection, a statistical test on weighted residuals, ie, the weighted difference between data and model prediction, is available, ie, the run test, to check for presence of model misfitting. In fact, since the sequence of the residuals can be viewed as an approximation of the measurement error sequence, one expects them to be independent; nonrandomness in the residuals indicates that the model is too simple for the data, eg, one may need more compartments than those postulated. Clearly, if the model does not fit the data, one knows the reason: it is too simple. But how does one know that the model is too complex, that is, the system is overmodeled instead of undermodeled? Suppose, for instance, one has some bolus decay tracer data obtained in a steady-state system. Linear compartmental models are appropri-

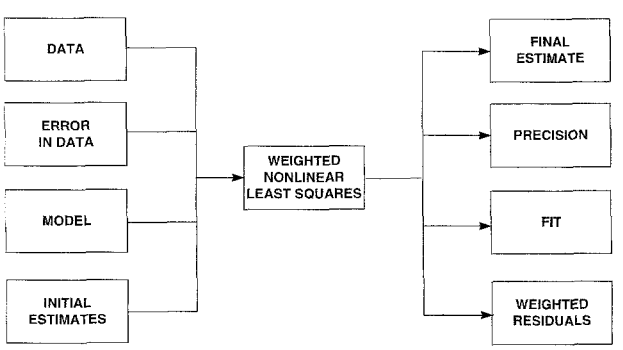

Fig 14. The ingredients of weighted nonlinear least squares from the user's point of view showing input and output.

ate and one describes the data with a one-, a two-, a three-, and a four-compartment model. How does one know the right model order? Clearly, residuals and indices like WRSS are not of help, since they will always improve as model order increases. One has to look at the covariance matrix of parameter estimates: precision of parameter estimates will clearly worsen as model order increases and parameters estimated with poor precision are a symptom of a model too complex for the data. So, in general, one has to find a good compromise between model fit to the data and precision of parameter estimates.

One speaks of parsimonious modeling and, at least for linear compartmental models, there are criteria such as the F test and the Akaike and the Schwarz criteria, which can be used if measurement errors are independent and gaussian. For instance, the Akaike (AIC) and Schwarz (SC) criteria, for the case of measurement error variances known or known up to a proportionality constant, with weights optimally chosen, are given by, respectively[12,37]:

$$AIC = WRSS + 2P; \qquad AIC = N \ln WRSS + 2P \tag{20}$$

$$SC = WRSS + P \ln N; \quad SC = N \ln WRSS + P \ln N \tag{21}$$

where P is the number of unknown parameters of the model and N is the number of data. The parsimonious model is the one which has the smallest value of AIC or SC.

Optimal Experiment Design

At this point, one has a compartmental model structure, a description of the measurement error, and a numerical value of the parameters together with the precision with which they can be estimated. It is now appropriate to address the *optimal experiment design* issue. The rationale of optimal experiment design is to act on design variables such as the number of test inputs and outputs, form of test inputs, number of samples and sampling schedule, and measurement errors, so as to maximize, according to some criterion, the precision with which the compartmental model parameters can be estimated.[12] The Fisher information matrix J, which is the inverse of the lower bound of the covariance matrix (equation 19), is treated as a function of the design variables, and usually the determinant of J (this is called D-optimal design) is maximized in order to maximize precision of parameter estimates, and thus numerical identifiability.

The optimal design of sampling schedules, ie, the determination of the number and location of discrete time points where samples are collected, has received much attention as it is the variable that is less constrained by the experimental situation. Theoretical and algorithmic aspects have been studied,[38-40] and software is available for linear and nonlinear compartmental models with a multiinput-multioutput experimental configuration.[40] Optimal sampling schedules are usually obtained in an iterative manner. One starts with the model obtained from pilot experiments, and the algorithm computes the optimal sampling schedule for subsequent experimentation. An important result for single-output linear compartmental models is that D-optimal design usually consists of independent replicates at P distinct time points, where P is the number of parameters to estimate. Replicates allow to improve the precision of the parameter estimates (the CV of parameter estimates improves by a factor of $\sqrt{m}$ if m are the replicates).

Optimal sampling schedule design has been shown to improve precision as compared with schedules designed by intuition or other convention[41]; to optimize the cost effectiveness of a dynamic clinical test by reducing the number of blood samples withdrawn from a patient without significantly deteriorating their precision[42,43]; and to obtain less dispersion in population parameter estimates.[38]

The optimal input design problem has been relatively less studied, but some results are available on equidose rectangular inputs (including the impulse) for parameter estimation in compartmental models.[44-46]

INPUT-OUTPUT MODELING

Often, compartmentalizing the system as discussed earlier may turn out too demanding or simply not necessary. Consider the steady-state case first. Suppose, eg, one needs to measure endogenous glucose production of an individual in the basal steady-state, and not the fluxes and masses of glucose in the body. Then, one resorts to a tracer experiment in order to not perturb the basal steady-state, and depending on the chosen tracer administration format, one can calculate endogenous glucose production (EGP) with the well-known formulas[12] (see also equations 33 and 34):

$$EGP = u \cdot C/c \tag{22}$$

$$EGP = \frac{d \cdot C}{\int_0^\infty c(t)\, dt} \tag{23}$$

for the primed constant infusion and the bolus experiment, respectively: u is the tracer constant infusion, d the bolus dose, and c and C, the tracer and tracee concentration, respectively.

The same demand also applies in non–steady-state, eg, suppose one has to measure endogenous glucose production or insulin secretion after a meal, but is not interested in a detailed structural picture of in vivo glucose or insulin kinetics.

All of these problems are input estimation problems (Fig 15), ie, one is not able to measure directly the inputs, eg, insulin secretion rate or endogenous glucose production, but only their causally related effects in the circulation, ie, the time course of the concentration of the substance in plasma. There is thus the need to reconstruct the unknown causes from the measured effects. This problem is often called an inverse problem, ie, while a direct problem is a problem oriented along the cause-effect chain, an inverse problem is associated with the reversal of this chain.

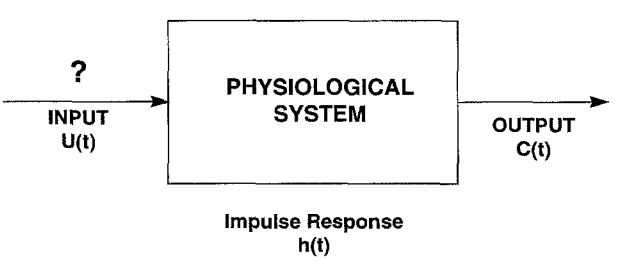

Fig 15. The inverse problem.

Consider a linear time-invariant system, eg, a hormone with linear and time-invariant kinetics. The input estimation problem (Fig 15) can be attacked by considering the following integral equation[12]:

$$C(t) = \int_0^t h(t - \tau)U(\tau)\, d\tau \qquad (24)$$

where U is the (unknown) input and C is the (measurable) output of the system. The function h describes the input-output behavior of the system; it is called the impulse response of the system and represents the time course of the output when the system is forced by a unitary bolus input at time 0.

Usually only sampled noisy measurements are available (see equation 16):

$$C^{obs}(t_i) = C(t_i) + E(t_i) \quad i = 1, \ldots, N \qquad (25)$$

where E denotes the measurement error affecting the observations.

The input estimation problem amounts to reconstructing the input U given h and the measurements $C^{obs}(t_i)$, and since the right-side term of equation 24 is a convolution product, it is best known as a *deconvolution* problem.

When the system is in steady-state (U and C constant in time) the solution of the input estimation problem is straightforward, ie, equation 24 becomes an algebraic equation (time t in the integral sign goes to infinity) which can be easily solved for the unknown input U. The formulae of equations 22 and 23 are examples of the particularization of equation 24 to the glucose system.

When the system is in non–steady-state (U and C vary in time), the problem is difficult to solve, since inverse problems as equation 24 are well known to be ill-posed, ie, it does not admit a unique solution. It is worth noting that the physiological setting offers additional difficulties with which one has to cope: ill-conditioning, ie, a small percent error in the measured output can result in a much greater percent error in the estimated input; measurement error of the data and uncertainty of the impulse response (it has to be estimated from experimental data); nonuniform and/or infrequent sampling; and inputs are intrinsically nonnegative.

To face ill-posedness and ill-conditioning, two major approaches have been proposed: parametric and nonparametric deconvolution. *Parametric* methods assume that the input has a given functional expression depending on a small number of parameters; in this way, the input estimation problem is restated as a parameter estimation problem that can be solved by using the nonlinear least squares technique discussed previously. However, this approach involves strong assumptions concerning the shape of the input, which makes it difficult to apply in practice and to handle, eg, confidence limits and nonnegativity constraints. *Nonparametric* methods do not require the postulation of a functional form of the input and simply exploit the available a priori (quantitative) knowledge of its regularity. The problem is how to obtain, under these circumstances, a statistically sound estimate of the input and its confidence intervals by means of a computationally efficient algorithm. Recently, the regularization method, which exploits prior information on the smoothness of the input by imposing appropriate penalties on its derivatives, has been put in a stochastic embedding.[47] This has allowed one to place the choice of the regularization parameter, which weights the role of the a priori information in determining the input estimate, on firm statistical grounds. Of note is that the method allows the reconstruction of the input, with its confidence intervals, in virtually continuous time. We refer to De Nicolao et al[47] for the theory and numerical aspects of the deconvolution algorithm.

In formulating the input estimation problem (equation 24), we have assumed the system to be linear and time-invariant. This means that the impulse response h can be described by a model of data not by a model of system, eg, a compartmental one. Usually a good candidate model of g is:

$$h(t) = \sum_{i=1}^{M} A_i e^{-\alpha_i t} \qquad (26)$$

where $\alpha_i \geq 0$.

To determine the impulse response, the ideal probe is a tracer. When tracers are not available or cannot be used, one has to perturb the system with an exogenous input of the substance of study. This is not without problems, since linearity can be violated and feedback inhibition mechanisms may be triggered. Often a "tracer-like" situation is recreated by inhibiting the endogenous input flux (eg, a somatostatin infusion is usually employed to inhibit insulin secretion) or by determining the impulse response in a pathological state where no endogenous input flux is present (assuming the kinetics are not affected by the pathology). The nonlinear least-squares parameter estimation machinery described in the previous section can be used to determine the model order (how many exponentials) and the estimates of A_i and α_i with their precision.

If the system is linear, but time-varying, equations 24 and 26 do not apply. In this case, the response h to a unitary bolus given at τ_0 depends on the particular value of τ_0 and the input estimation problem translates into the one of solving a Fredholm integral equation of the first kind:

$$C(t) = \int_0^t h(t, \tau)U(\tau)\, d\tau \qquad (27)$$

The function g depends on both t and τ and not only on their difference like in equation 24. To describe g, a model of system, eg, a compartmental one described by equation 3 or 12, is needed for a tracee or a tracer experiment, respectively. An example of equation 27, which will be discussed later, deals with the estimation of endogenous glucose production during an IVGTT: the function g of equation 27 for the glucose system in this situation can be obtained via a linear two-compartment model with time-varying parameters.[6] It is worth noting that the theory and deconvolution algorithm[47] discussed for solving equation 24 also works with equation 27.

MODEL VALIDATION

It is not difficult to build model of systems—the difficulty lies in making them good and reliable for answering the question asked. For the model to be useful, one has to have confidence in the results and predictions that are inferred from it. Such confidence can be obtained by *model validation*. In other words, validation involves assessing whether the model is adequate for

its purpose. This is a difficult and highly subjective task in modeling of physiologic systems, because intuition and understanding of the system, among others, play an important role. It is also difficult to formalize related issues such as model credibility, ie, the use of the model outside its established validity range. Some efforts have been made, however, to provide some formal aids for assessing the value of models of physiological systems. In particular, validity criteria and validation strategies of models of physiological systems are available[48] that take into account both the complexity of the model and the extent of available experimental data. Of particular importance is the ability to validate a model-based measurement of a system parameter, obtained, eg, by a compartmental model or by an input-output deconvolution model, by an independent experimental technique. A model that is valid does not mean it is true; all models have a limited domain of validity and it is hazardous to use a model outside the area it has been validated for.

A valid model cannot only be used to measure nonaccessible parameters, but also for simulation. Suppose one wants to see how the system behaves under certain stimuli, but it is inappropriate or impossible to carry out the experiment on the system. If a valid model of the system is available, one can perform an experiment on the model, eg, by using a computer to see how the system would have reacted. This is called *simulation.* Simulation is thus an inexpensive and safe way to experiment with the system. Clearly, the value of the simulation results depends completely on the quality, ie, validity, of the model of the system.

GLUCOSE FLUXES

Now that we have a good appreciation of the basic tools of modeling methodology, it is possible to attack the nonaccessible system parameter problem in practice. As anticipated, our proof of the pudding is the glucose-insulin system of Fig 5, so, we will start with the measurement of glucose fluxes, then proceed to that of insulin fluxes, and finally attack the measurement of glucose-insulin signaling.

We assume that the glucose system can be described by a compartmental model with time-varying parameters. The model has an accessible pool (usually blood) that exchanges with other nonaccessible compartments. In general, there may be glucose fluxes taking place in the accessible, as well as in the nonaccessible compartments. It is useful to use a different notation to distinguish between fluxes pertaining to the accessible pool and those pertaining to the whole system. Ra (rate of appearance) will denote the rate of de novo entry of glucose in the accessible pool and Rd (rate of disappearance), the net glucose outflux from the accessible pool (resulting from the glucose exchange between the accessible and nonaccessible pools). Ra and Rd are related by the mass balance equation of the accessible pool (labeled as pool 1):

$$\frac{dQ_1}{dt} = Ra(t) - Rd(t) \tag{28}$$

where $Q_1 = C_1 \cdot V_1$ is the glucose mass in the accessible pool (C_1 is glucose concentration and V_1 is the volume of the accessible pool). As far as the whole glucose system is concerned, EGP will denote endogenous production of glucose and U, whole-body glucose uptake. EGP and U are related by the mass balance equation of the whole system:

$$\frac{dQ_T}{dt} = EGP(t) - U(t) \tag{29}$$

where $Q_T(t) = \Sigma_{i=1}^{n} Q_i(t)$ is the total mass of glucose in the system. Which is the relationship between accessible pool and whole-body glucose fluxes? Since endogenously released glucose enters the hepatic and renal veins, Ra well measures with EGP (plus any exogenous glucose input, when present). In contrast, since glucose can be utilized by tissues in both the accessible and nonaccessible pools, Rd is, in general, different from U.

It is easy to realize that it is not possible to determine Ra, EGP, Rd, and U relying only on measurements of plasma glucose concentration. This requires the administration of a glucose tracer. In fact, since there is no endogenous source of tracer, one can segregate glucose production from glucose uptake. How to obtain the glucose fluxes from tracer data can be easily appreciated by resorting to the concept of impulse response. Determination of input and output glucose fluxes from tracer data can be obtained by an input-output modeling approach. The relationship between the glucose input to the glucose system, Ra, and the glucose concentration measured in plasma, C_1, is given by the convolution integral:

$$C_1(t) = \int_0^t h(t, \tau)Ra(\tau)\, d\tau \tag{30}$$

where $h(t, \tau)$ is the impulse response of the glucose system. Due to the tracer-tracee indistinguishability principle, the impulse response of the tracer coincides with that of the tracee. Calculation of $h(t, \tau)$ from tracer data is easy in steady-state, but difficult in non–steady-state. In fact, in steady-state, $h(t, \tau)$ is the impulse response of a linear system and can be determined virtually in a model-independent fashion, as discussed in the section Input-Output Modeling. In contrast, in non–steady-state, the glucose system is linear, but time-varying, and thus calculation of $h(t, \tau)$ requires postulation of a structural model of glucose the system. In the following sections, we will detail how Ra, EGP, Rd, and U can be calculated in both steady- and non–steady-state conditions.

Steady-State

Whole-body modeling. In steady-state, glucose masses and fluxes in the system are constant. The mass conservation principle applied to the accessible pool and to the whole system states that:

$$Ra = Rd \tag{31}$$

$$EGP = U \tag{32}$$

Calculation of Ra from equation 30 is straightforward, because, since the glucose system is linear and time-invariant, its impulse response is a sum of exponentials. Parsimony criteria like the Akaike information criterion allow the selection of the appropriate order of the exponential response. Two exponentials are

necessary and sufficient to accurately describe the impulse response in humans.[1] Once h(t, τ) is known, Ra is calculated as:

$$Ra = \frac{d \cdot C_1}{\int_0^\infty c_1(\tau)\, d\tau} = \frac{d \cdot C_1}{\sum_{i=1}^{2} \frac{A_i}{\alpha_i}} \tag{33}$$

where d is the dose of the tracer bolus injection, c_1 is plasma tracer concentration, and A_1, A_2, α_1, and α_2 are the coefficients and eigenvalues, respectively, of the two-exponential function that fits data.

Often, the tracer is administered as a primed continuous infusion. At the end of the tracer equilibration period, a constant tracer concentration is attained in plasma. Under such experimental conditions, thanks to the tracer-tracee indistinguishability principle and to the linearity and time-invariance of the glucose system, one can write:

$$R_a = u_1 \frac{C_1}{c_1} \tag{34}$$

where u_1 denotes the constant rate of tracer infusion. Once Ra is known, Rd and U can be calculated.

This approach to the calculation of glucose fluxes in steady-state can be applied to investigate the glucose system not only in the basal, but also in another steady-state attained by some experimental manouver. For instance, using the hyperinsulinemic-euglycemic clamp, the glucose system can be brought from the basal to another steady-state characterized by basal glucose, but elevated insulin. In this way, one can investigate the effect of insulin alone on glucose fluxes. This has been done by Cobelli et al,[1,2] where the impulse response of glucose has been studied with a tracer injection both in the basal and in the elevated insulin state. Using structural modeling, one can gain a better comprehension of the insulin effect on glucose kinetics, but this requires development of a model based on physiological knowledge. A compartmental model of glucose kinetics has been proposed and identified from tracer data before and at the end of the euglycemic-hyperinsulinemic glucose clamp.[1,2] If the very early samples (0 to 2 minutes) are neglected, a two-compartment model describes the data best.[1] The volume of the accessible pool is 158 mL/kg, and thus comprises not only plasma (≈46 mL/kg), but also the glucose-consuming tissues that exchange rapidly with plasma, ie, red blood cells, liver, kidneys, and CNS. Of note is that these tissues consume glucose in a virtually insulin-independent fashion. The nonaccessible glucose pool pertains to tissues like muscle and fat muscle that equilibrate more slowly with plasma. These tissues consume glucose in an insulin-dependent way. This brought us to postulate the model, shown in Fig 16, with two irreversible losses: one, insulin-independent and pertaining to the accessible pool, and the other, insulin-dependent and associated with the remote glucose pool. This choice also ensured a priori unique identifiability of the model, because one can take advantage of the notion that at basal steady-state, insulin-independent glucose uptake is three times the insulin-dependent one. This provided the constraint among the model parameters that made the model a priori uniquely identifiable. When the model was identified in the hyperinsulinemic state, it become apparent that

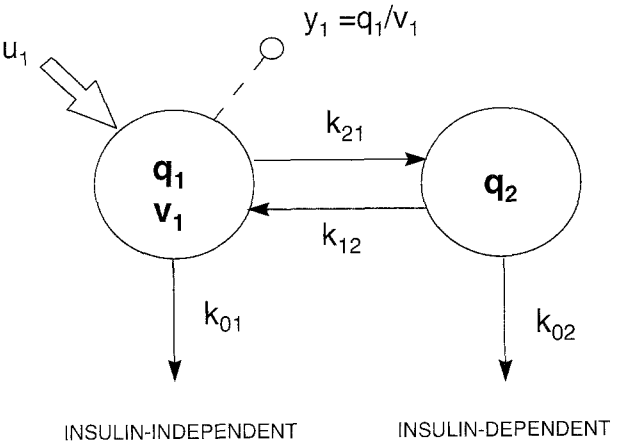

Fig 16. Two-compartment model of tracer glucose kinetics.

not only the irreversible loss in the remote glucose pool increases, but also the rate constants that describe the glucose exchange between the two compartments change.

Regional modeling. Whereas the model of Fig 16 describes steady-state glucose kinetics at the whole-body level, compartmental models also help to better understand kinetic events inside an organ or a tissue, ie, at the regional level. Of course, to develop a model of glucose kinetics at the regional level, measurements at the regional level are needed. The most widely used regional experimental approaches fall into two major categories: *tracer-balance* techniques and *residue function* techniques. To the first belongs the multiple tracer dilution technique, and to the second, positron emission tomography (PET) and nuclear magnetic resonance (NMR). Below, we focus on human skeletal muscle (see Bonadonna et al[49] for a review of both experimental and modeling aspects) and discuss the multiple tracer dilution and PET modeling-based measurements of glucose transport and phosphorylation.

The *multiple tracer dilution* technique. (Fig 17) is based on the simultaneous pulse injection at the inlet of the organ of multiple tracers with different molecular characteristics and on the measurement at the organ outlet of their washout curves. The approach developed by Saccomani et al[50] for measuring glucose transport and phosphorylation in the human skeletal muscle is a "three-tracer approach" based on injecting in the forearm of the subject an extracellular tracer (D-[^{12}C] mannitol), one transportable but not metabolizable (3-*O*-[^{14}C]-methyl-3-D-glucose]) tracer, and one permeant and metabolizable (D-[3-

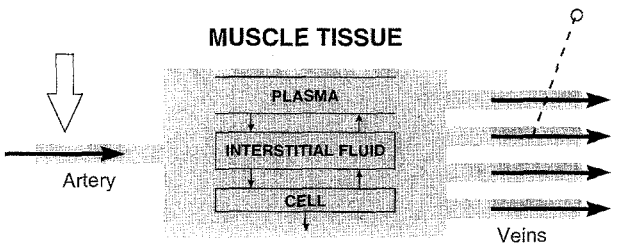

Fig 17. The multiple tracer dilution experiment in the muscle tissue. A number of different tracers are simultaneously injected at the inlet of the organ and their washout curves are measured at the outlet.

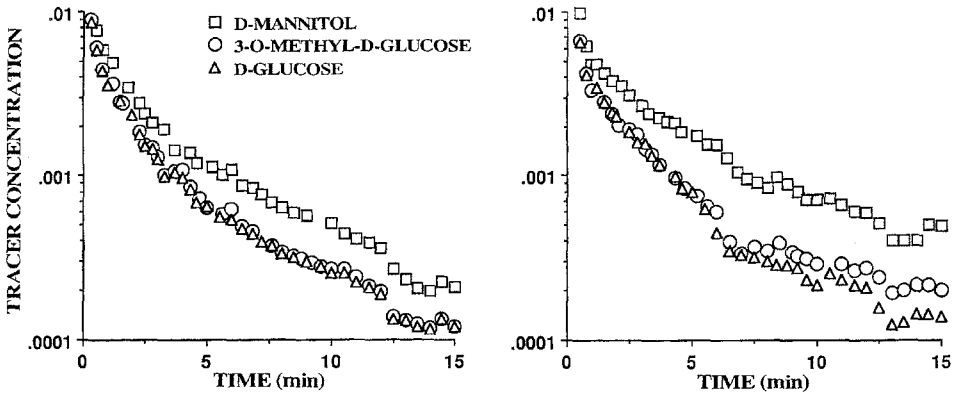

Fig 18. Washout curves of mannitol, 3-*O*-methyl-D-glucose and D-glucose tracers in basal state (A) and during hyperinsulinemia (B) in the human skeletal muscle. Tracer concentrations are normalized to respective doses and expressed in a logarithmic scale. Reprinted with permission.[50]

^{3}H]glucose) tracer. The three tracer dilution curves (Fig 18) are then analyzed with the compartmental model of Fig 19, which describes blood-flow heterogeneity, glucose transport, and phosphorylation. Briefly, compartments 1 and 8 denote the sites of input and measurement, respectively; compartment 15 represents erythrocytes; compartments 2 through 7 represent plasma plus interstitial fluid; and compartments 9 through 14 are cellular compartments. Irreversible loss of the tracers takes place from the sampling compartment, the injected compartment, and the erythrocyte pool, with the latter two accounting for the fact that only a fraction of the injected dose reaches the sampling compartment. An additional irreversible loss for D-[3-^{3}H]glucose only takes place from each of the cellular compartments that describes intracellular metabolism. The uniquely identifiable parameterization of the tracer model includes k_{in}, k_{out}, k_{met} (min^{-1}), which measure transmembrane inward transport, transmembrane outward transport, and phosphorylation, respectively. Other important kinetic parameters

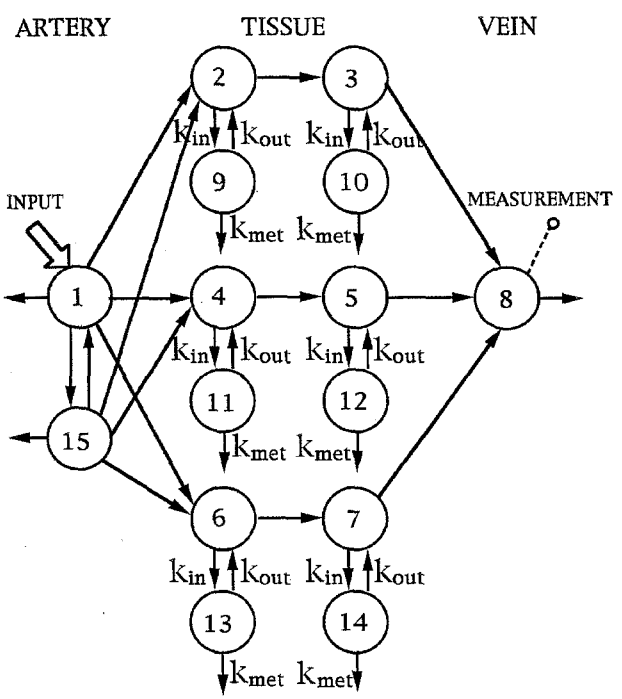

Fig 19. Tracer model for interpreting the washout curves of Fig 18. Reprinted with permission.[50]

are the mean transit time of a D-mannitol and 3-*O*-methyl-3-D-glucose molecule. Having quantified the tracer model, the tracee model can be solved if the arterial glucose flux is assumed known (blood flow is measured). Several kinetic parameters can be estimated. The extracellular, Q_{ec}, and intracellular glucose, Q_{ic}, masses (mmol) are given by:

$$Q_{ec} = Q_2 + Q_3 + Q_4 + Q_5 + Q_6 + Q_7 \quad (35)$$

$$Q_{ic} = Q_9 + Q_{10} + Q_{11} + Q_{12} + Q_{13} + Q_{14} \quad (36)$$

where Q_2 through Q_{14} denote the glucose masses in compartments 2 through 14.

The inward and outward transmembrane glucose fluxes, F_{in} and F_{out}, and the phosphorylation glucose flux, F_{met}, (mmol/min) are given by:

$$F_{in} = k_{in}Q_{ic} \quad (37)$$

$$F_{out} = k_{out}Q_{ic} \quad (38)$$

$$F_{met} = k_{met}Q_{ic} \quad (39)$$

Finally, one calculates the extracellular, V_{ec}, and intracellular, V_{ic}, volumes (mL) and thus the extracellular, C_{ec}, and intracellular, C_{ic}, concentrations (mmol/mL) as:

$$C_{ec} = Q_{ec}/V_{ec} \quad (40)$$

$$C_{ic} = Q_{ic}/V_{ic} \quad (41)$$

This model-based measurement has been applied to study the effect of insulin on glucose processes inside the muscle tissue[50] and to identify defective steps of glucose kinetics in non–insulin-dependent diabetes mellitus (NIDDM).[51]

The *PET technique* is based on the injection of radioactive molecules labeled with positron-emitting nuclides with subsequent tomographic detection of the radioactive nuclide within the organ of interest (Fig 20). The typical protocol for the study of glucose transport and phosphorylation in human muscle involves the pulse injection of a tracer amount of [^{18}F]-fluoro-deoxy-glucose ([^{18}F]FDG) in a peripheral vein and the frequent measurement of arterialized FDG concentration and of FDG tissue activity.[52] Dynamic PET data are usually analyzed with a three-compartment model exhibiting three[53] or four[54] rate

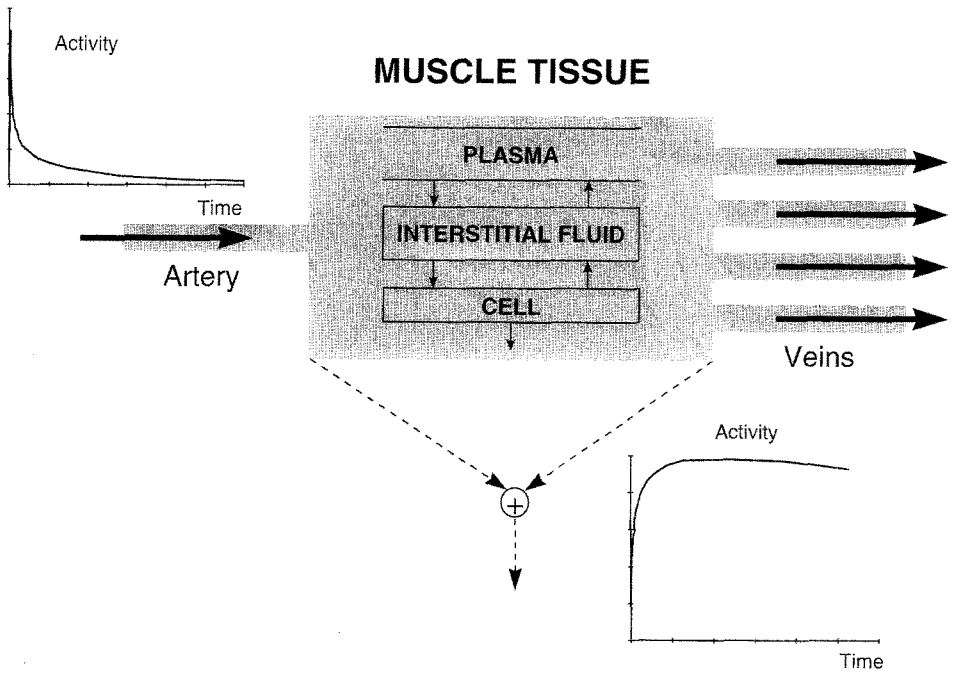

Fig 20. PET experiment in the muscle tissue.

constants. The model of Sokoloff et al[53] is shown in Fig 21 and is described by:

$$\dot{q}_2(t) = k_{21}c_1(t) - (k_{12} + k_{32})q_2(t), \quad q_2(0) = 0$$
$$\dot{q}_3(t) = k_{32}q_2(t), \quad q_3(0) = 0 \qquad (42)$$
$$y_1(t) = (1 - v_{bt})[q_2(t) + q_3(t)] + v_{bt}q_1(t)$$

where c_1 is arterial FDG tracer concentration ($c_1 = q_1/V_1$, where q_1 is FDG tracer mass and V_1 is the volume of compartment 1); q_2 is free FDG tracer mass in the interstitial fluid and in the tissue (compartment 2); q_3 is FDG-6-phosphate tracer mass in the tissue (compartment 3); k_{21} (mL/min^{-1}), k_{12}, and k_{32} (min^{-1}) are rate parameters; v_{bt} is the vascular volume present in the tissue; and y is the PET dynamic measurement. Note that there is no mass balance equation for compartment 1, because the measured arterial tracer concentration c_1 acts as model input.

Since all of the parameters, k_{21}, k_{12}, k_{32}, and v_{bt}, can be estimated, a PET study can quantitate the FDG rate constants of inward and outward transport and phosphorylation. Kelly et al[52] have studied the effect of insulin on the FDG rate constants in both normal and NIDDM subjects.

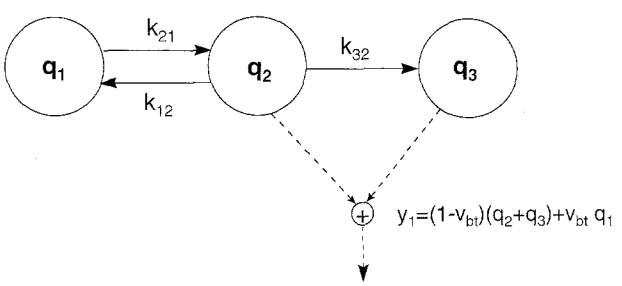

Fig 21. The 3-rate constants model for interpreting PET [^{18}F]FDG dynamic data.

An important assumption made in the model is that the tissue fractional extraction of FDG from the blood is small (<5%). This assumption, which is reasonable if the organ under study is the brain under conditions of euglycemia or hyperglycemia, or skeletal muscle in the postabsorptive state, is not fulfilled in muscle during hyperinsulinemia, when fractional extraction may be as high as 30% to 40% in insulin-sensitive individuals. Whether, and to what extent, high fractional extractions can affect the estimates of k_{21}, k_{12}, and k_{32} is presently unknown.

It must also be remembered that the estimated FDG parameters cannot be applied directly to glucose, because deoxyglucose is an analog, and not an ideal tracer, ie, both the transporter and hexokinase do not handle glucose and deoxyglucose with the same efficiency. Thus, the estimates of FDG k_{21}, k_{12}, and k_{32} can at best provide semiquantitative information on glucose transport and phosphorylation. This also prevents the quantitation of the glucose masses of the tracee model and, thus, for instance, of fluxes of equations 37 to 39. Usually, one calculates the rate of glucose phosphorylation as:

$$F_{met} = \frac{k_{21}k_{32}}{k_{12} + k_{32}} \frac{C}{LC} \qquad (43)$$

where C is glucose concentration and LC is the lumped constant, a factor that accounts for the kinetic differences between glucose and deoxyglucose in transport and phosphorylation. However, the assumption is made that LC is known and the same in different individuals, in different pathological conditions and in different experimental manouvers. At present, an accurate study on LC values in muscle tissue in various situations, eg, elevated insulin states, is still lacking.

Finally, it should be noted that, gauging the individual steps of glucose transport and phosphorylation from a single-tracer study is difficult, because the information content of the data is

limited, and the interpretative model must necessarily be simple.

Non–Steady-State

Estimation of Ra and EGP. In non–steady-state, Ra is a function of time and its estimation takes place in two steps. First, the impulse response is identified from tracer data and then Ra is reconstructed from the impulse response and tracee data by solving the integral equation (equation 30). In non–steady-state, the impulse response cannot be determined unless a model of the system is formulated. This means that not only a model structure must be postulated, but there is also the need to indicate which parameters are subjected to variations during the non–steady-state and specify how these variations occur. Different models will lead to different estimates of Ra.

The model that is widely used for non–steady-state analysis is the one proposed by Steele et al.[55] This model does not intend to be an accurate description of the glucose system, but a simple computational tool applicable to any non–steady-state situation. Steele's model is monocompartmental, with a time-varying irreversible loss that can be assessed from tracer data, thus making the time-varying impulse response $h(t, \tau)$ perfectly known. Then, Ra can be calculated from $h(t, \tau)$ and tracee data via the integral equation (equation 30). Specifically, the computation of Ra can be performed with a direct formula in which the specific activity, ie, the tracer-to-tracee ratio, plays a key role. Steele's model is attractive, because it is simple and easy to implement. However, it has become apparent that it leads to erroneous conclusions. For instance, Steele's model predicts negative values of EGP during a euglycemic-hyperinsulinemic clamp[56-58] and an unphysiological jump of EGP above the baseline during the early part of an IVGTT.[6] The domain of validity of Steele's model has been analyzed theoretically and has been shown to be limited by the gross approximation inherent to its single-compartment structure.[59]

Tracer experiments in steady-state have shown that the description of the impulse response of the glucose system requires at least two exponentials, implying that glucose distributes not only in the accessible compartment, but also in a second, nonaccessible compartment. The two-compartment model proposed by Radziuk et al[60] embodies this physiological knowledge. Radziuk's model has been proposed in two versions (Fig 22): the first (Fig 22A) has a time-varying irreversible loss in the first compartment, $k_{01}(t)$, and assumes no irreversible loss in the second, nonaccessible compartment; the second (Fig 22B) has equal time-varying losses from both compartments $[k_{01}(t) = k_{02}(t)]$. The use of this model requires the preliminary estimation of V_1, k_{21}, and k_{12}, and of the basal value of k_{01} ($k_{02} = k_{01}$ for the second model version). These estimates can be obtained from tracer data generated by administering a tracer (usually as a primed continuous infusion) before the beginning of the non–steady-state. During the non–steady-state, the profile of the time-varying parameter can be calculated from the model equations after smoothing of the tracer data. It has been shown that Radziuk's model performs better than Steele's model,[60] even though margins of improvement are present.[61] This is due to the fact that Radziuk's model is still a general-purpose computational tool, rather than being a physiologically based description of the glucose system in non–steady-state. To appreciate the difficulties inherent to the formulation of a two-compartment model for the interpretation of non–steady-state, one must remember that there is an infinity of alternative structures that can describe equally well tracer data in steady-state. The difficult task is to decide where the irreversible glucose losses are placed (in only one of the two compartments or in both) and decide which parameters are subjected to vary in non–steady-state. In doing so, one is faced with a priori identifiability problems, even in steady-state. For instance, a model with irreversible losses in both compartments is not a priori identifiable (Fig 12) unless a constraint is used. Thus, the formulation of an adequate model of general use is not possible, and satisfactory solutions exist only in specific experimental situations. One of these cases is the euglycemic-hyperinsulinemic clamp. We have previously discussed that a two-compartment, physiologically based model of glucose kinetics can be identified both before and the end of the clamp, when a new equilibrium is attained. With these two snapshots of the system available, which allow a numerical picture of the model at the beginning and at the end of the clamp, it becomes possible to describe non–steady-state glucose kinetics during the perturbation. This is accomplished by allowing the three time-varying parameters, ie, the irreversible loss in the nonaccessible compartment and the exchange rates between the compartments, to change from their initial to their final values. This model represents an improvement on Steele's and Radziuk's models, because it provides estimates of EGP during the clamp that are more reliable than those provided by the other two models.[59] However, since the model has three time-varying parameters, it is difficult to employ it in non–steady-state situations different from the clamp. In addition, even during a clamp, care must be exercised to ensure that the tracer is infused in such a way that allows estimation of the initial and final model parameter configuration. A simplified version of this model has been formulated to interpret glucose kinetics during an IVGTT.[6] Insulin was assumed to control parametrically the irreversible loss of glucose from the second compartment, while the exchange rates between the two compartments were assumed to remain constant. By using this model to describe the time-

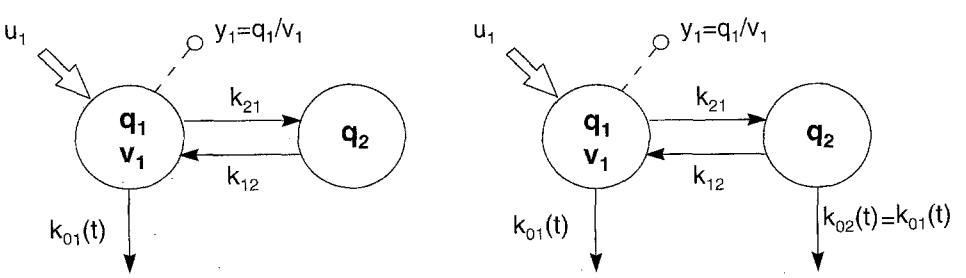

Fig 22. Two-compartment time-varying models of tracer glucose kinetics for interpreting non–steady-state data. One of the models (A) exhibits only a single time-varying irreversible loss parameter $k_{01}(t)$, while the other (B) has 2, with the constraint $k_{01}(t) = k_{02}(t)$ to guarantee a priori identifiability.

varying impulse response of glucose kinetics during the IVGTT, a profile of EGP was obtained by deconvolution that resulted in a far more reliable one than that provided by Steele's model.[6] Recently, the model prediction of EGP has been validated against the EGP profile obtained in a virtually model-independent fashion with the tracer-to-tracee ratio clamp technique in a dual stable isotope tracer study.[62,63]

Non–steady-state theory[59,64,65] indicates that the accuracy of the model reconstruction of Ra can be enhanced if the tracer is infused in such a way to reduce the changes in tracer specific activity, sa (or tracer-to-tracee ratio if a stable isotope tracer is employed), during the experiment. Ideally, if the tracer infusion, u(t), is adjusted so as to produce a constant specific activity throughout the experiment, Ra, is accurately estimated by:

$$Ra(t) = \frac{u(t)}{sa} \tag{44}$$

It is thus useful for the investigator to try to clamp the specific activity at a constant level by changing the tracer infusion rate in a suitable way. Even though the chosen format of tracer infusion is not exact so as to maintain the specific activity perfectly constant, a reduction in the magnitude of the derivative of specific activity, with respect to a conventional constant tracer infusion, will provide an estimate of Ra much less dependent on the validity of the model used.

The problem is how choose the correct administration format for u(t). To keep specific activity constant, u(t) should have the same shape (proportional) of the unknown Ra. Since Ra is the sum of the rate of appearance of exogenous glucose and EGP, it is evident that u(t) should not be kept constant, but should be varied during the experiment. Of note is that the rate of exogenous glucose appearance, when present, may or may not be known. For instance, during a euglycemic-hyperinsulinemic clamp, it is known, since it is the glucose infusion rate. In contrast, it is unknown (and to be estimated) during an OGTT or a meal when the rate of exogenous glucose is the rate of glucose absorbed from the gut and delivered in the peripheral circulation after passage through the liver. In any case, the measured glucose concentration is the sum of two components, exogenous glucose, C_{ex} (due to exogenous sources), and endogenous glucose, C_{end} (due to EGP):

$$C(t) = C_{end}(t) + C_{ex}(t) \tag{45}$$

The distinction between C_{end} and C_{ex} plays a key role and provides a general approach for clamping of specific activity. In fact, to minimize the changes in specific activity, the tracer could be infused in such a way to clamp the exogenous and the endogenous specific activity separately. Clamping the exogenous glucose specific activity is simple: one has to add some tracer to the exogenous infusate. Clamping the endogenous component is more difficult, since one has to change the basal constant rate of tracer infusion in such a way to mimic the expected time course of EGP during the experiment. This may sound like circular reasoning, since adjusting the tracer infusion rate requires the knowledge of EGP, which is exactly what one is trying to determine. However, usually some a priori information about the behaviour of EGP when the system is displaced from the steady state is available and this allows one to smooth out the brisk or large changes in specific activity. This leads to the concept of sequential design of the tracer infusion rate: the first trial can be verified later by measuring specific activity, and if one misses the goal, one can learn from the error and improve the format of tracer administration in the subsequent experiment. In practice, in the first experiment, one should use an administration format dictated by a priori knowledge and intuition. The time course of specific activity will tell whether the specific activity clamp has been successful or not and will allow the investigator to refine the tracer infusion rate to be used in the subsequent experiment. This procedure can be repeated a few times, as long as a satisfactory format is obtained. This strategy has been recently used with success in humans for the estimation of EGP after a mixed meal.[3]

Estimation of Rd and U. In non–steady-state, Rd and U are no longer equal. U equals the sum of all the glucose fluxes irreversibly leaving the system:

$$U(t) = \sum_{i=1}^{n} k_{0i}(t)Q_i(t) \tag{46}$$

where n is the number of compartments of the model of the system. Rd can be expressed in terms of compartmental fluxes as follows:

$$Rd(t) = \sum_{\substack{i=0 \\ i\neq 1}}^{n} \Phi_{i1}(t) - \sum_{i=2}^{n} \Phi_{1i}(t) \tag{47}$$

where ϕ_{ij} is the flux from compartment j to compartment i, and ϕ_{01} is the irreversible loss from compartment 1. It is clear that the assessment of both Rd and U depends on the accuracy of the model used to represent the glucose system. Nevertheless, it is easy to recognize that the assessment of Rd is less problematic than that of U, because of the different relationship that these two fluxes have in relation to Ra:

$$Rd(t) = Ra(t) - dQ_1(t)/dt \tag{48}$$

$$U(t) = Ra(t) - dQ_T(t)/dt \tag{49}$$

Both Rd and U can be derived from Ra, which, as shown above, can be accurately estimated, even with an approximate model, by resorting to the specific activity clamp. However, whereas the estimation of Rd only requires measurement of the rate of change of the glucose mass in the accessible pool only, estimation of U requires knowledge of the rate of change of the glucose mass also in the nonaccessible compartments. Thus, whereas Rd can be accurately measured if specific activity is kept constant and the volume of the accessible pool is known, estimation of U requires a model of the system (accessible and nonaccessible). Estimation of Rd is thus relatively easy, since there is no need to postulate a model of the (nonaccessible) system. However, the calculation of Rd is also important, because its knowledge allows inferences concerning the time course of U. For instance, if the glucose system moves from steady-state into a non–steady-state period, and then returns to the former steady-state, the following relationship between Rd and U holds[66]:

$$AUC[Rd(t)] = AUC[U(t)] \tag{50}$$

where AUC denotes the area under the curve. A more specific relationship between the time courses of Rd and U during the non–steady-state can be derived if one assumes that the only time-varying parameter is the irreversible loss of the accessible pool. Under these circumstances, for a system that goes into a non–steady-state period in which glucose concentration increases, one has:

$$Rd(t) > U(t) \tag{51}$$

Conversely, for a system that goes into a period in which glucose concentration decreases, one has:

$$Rd(t) < U(t) \tag{52}$$

INSULIN FLUXES

Insulin level in plasma is a function of three processes: insulin secretion by the pancreas, hepatic insulin extraction, and insulin kinetics. The same reasoning developed earlier for glucose also applies to insulin: fluxes occurring in the accessible pool such as Ra and Rd can be defined. Ra, in particular, will coincide with the systemic rate of appearance of insulin after its extraction by the liver. Similarly, rates of insulin secretion and degradation can be defined. In the following section, we will focus on modeling approaches to the quantitation of two major processes: insulin secretion and hepatic insulin extraction.

Insulin Secretion

The problem of assessing insulin secretion can be viewed as an input estimation problem, analogous to the one already discussed for the assessment of endogenous glucose production. However, assessment of the insulin secretion rate, ISR, is complicated by the presence of the liver that extracts insulin to a large and probably variable extent. This problem can be bypassed if C-peptide instead of insulin is used in solving the input estimation problem by deconvolution. C-peptide is equimolarly secreted with insulin, it is not extracted significantly by the human liver, and its kinetics have been shown to be linear and time-invariant for a large range of C-peptide concentrations.[67] In addition, evidence exists that the inhibition effect of C-peptide on its own secretion appears to be, if any, very small,[67,68] and that C-peptide kinetics are linear and time-invariant also in the presence of glucose and insulin concentrations that vary in time, like during a meal or an IVGTT or OGTT.[69,70] Strictly speaking, one reconstructs posthepatic C-peptide Ra; however, since the liver dynamics are very rapid, C-peptide Ra is a good measure of prehepatic C-peptide secretion, and thus of ISR. One can thus use deconvolution to reconstruct ISR both in steady- (equations 22 and 23) and non–steady- (equation 24) state. The estimation of ISR in non–steady-state, eg, during a meal or an IVGTT, requires the knowledge of the impulse response of the C-peptide system, g(t). This is usually obtained by a bolus injection experiment (but the input administration format depends on the problem being studied[71]) of synthetic human C-peptide with a concurrent infusion of somatostation to inhibit endogenous secretion. However, it is worth noting that the description of the impulse response of the C-peptide system does not require a compartmental model, but only an input-output one, ie, the exponential model of equation 26. Usually, a two-exponential model is employed,[72] but sometimes a three-exponential model has been reported to be the most parsimonious one.[73] If the impulse response cannot be obtained in the individual study, the normal population C-peptide kinetic parameters reported by Van Cauter et al[74] can be used as a reliable alternative for all those situations where renal function, and thus C-peptide kinetics, is not impaired. Deconvolution of C-peptide concentration profiles has been used extensively to reconstruct ISR in various physiopathological situations,[67,75,76] as well in clinical tests like intravenous and oral administration of glucose.[70,71,77,78]

Hepatic Insulin Extraction

Hepatic insulin extraction, HE, is related to ISR and posthepatic insulin Ra by the following expression:

$$HE(t) = \frac{ISR(t) - Ra(t)}{ISR(t)} \tag{53}$$

Thus, hepatic insulin extraction can be calculated by applying deconvolution to the C-peptide and insulin systems simultaneously. Assessment of insulin Ra by deconvolution requires the preliminary assessment of insulin kinetics. In this section, we will discuss how insulin kinetics can be assessed, first under the symplifying assumption that insulin kinetics are linear and, then, in the more general case, when linearity cannot be assumed.

Under the assumption that insulin kinetics are intrinsically linear within the range of insulin concentrations experimentally explored, insulin kinetics can be described by a linear model. If assessment of insulin kinetics is aimed at the calculation of posthepatic insulin delivery rate by deconvolution, an exponential input-output model (equation 26) is sufficient to describe the impulse response of the insulin system. Otherwise, if a more detailed picture of insulin distribution and degradation is desired, a compartmental model must be postulated. Several compartmental models of insulin kinetics have been published. Most of them have been reviewed previously.[79] The impulse response (or the compartmental model) can be identified, in the steady-state, using a tracer perturbation eg, an insulin tracer bolus. The use of an insulin tracer probe is not without problems and these have also been reviewed.[79] Briefly, insulin can be labeled with various radioactive isotopes of iodine or with tritium. Selectively labeled monoiodoinsulin of high specific activity can be obtained, but extreme care is needed to check the quality of the tracer. Tritiated insulin, albeit superior to iodoinsulin in terms of structural integrity, has a much lower specific activity and its administration fails a truly tracer situation, ie, it perturbs the system. Alternatively, a bolus of cold insulin can be employed, but one is faced with several critical issues. For instance, administration of nontrace amounts of insulin will induce hypoglycemia, unless a glucose clamp technique is used to prevent it. Hypoglycemia triggers circulatory and hormonal counterregulatory responses, which may affect insulin kinetics. Second, if insulin influences its own kinetics, the administration of cold insulin may shift the system into its nonlinear mode of operation (eg, saturation). Third, if insulin exerts feedback inhibition of its own secretion, it is necessary to distinguish between exogenously administered and endogenously produced

hormone. As a result, the observed insulin time course is the result of the contributions of both exogenous insulin administration and a time-varying endogenous insulin secretion. The latter component may confound kinetic analysis and lead to biased results. Somatostatin infusion has been suggested as a means to overcome this problem. Alternatively, one can single out the contribution of endogenous secretion to the observed insulin time course by using C-peptide kinetic modeling and deconvolution.

The domain of validity of the linearity assumption for the insulin system has also been reviewed.[79] A potential, important source of nonlinearity is saturation of hepatic insulin extraction. In investigating the linearity of insulin kinetics, exogenous insulin infusion rates are used and the resulting insulin levels attained in plasma are measured. Under these conditions, the liver is exposed to the same insulin levels measured in the peripheral circulation. Previous studies both in humans and in dogs have shown that the relationship between the insulin infusion rate and the corresponding insulin level fits a straight line up to peripheral plasma levels of 110 mU/mL. However, this result does not rule out the possibility that, under physiological conditions, nonlinearities may arise in the hepatic handling of insulin. For instance, during a meal, the liver is transiently exposed to high insulin concentrations due to the brisk increase of portal insulin levels. Therefore, hepatic insulin extraction may, at least in some species and under certain circumstances, be a function of insulin concentration even within the physiological range. Since hepatic extraction is the major component of insulin clearance, the nonlinearity seen at the liver site can influence insulin kinetics as well.[77,78] If the decrease in hepatic insulin extraction is small, it is likely that whole-body insulin kinetics will remain approximately linear. If the decrease is large, it can be also expected that the clearance rate of insulin will decrease in parallel. This means that insulin kinetics cannot always be safely assumed to remain linear and a more general approach is needed. Morishima et al[80] have proposed a two-compartment model of insulin kinetics with a time-varying irreversible loss from the accessible compartment that accounts for all of the nonlinearities and time changes that take place during a perturbation. The model has the same structure as one of the glucose models (Fig 21A) and its identification requires that an insulin tracer be infused throughout the experiment. Assessment of the basal value of the irreversible loss and of its time course during the non–steady-state is accomplished by using the parameter estimation techniques previously described for the assessment of non–steady-state glucose kinetics.

GLUCOSE AND INSULIN SIGNALING

Measuring parameters that describe glucose and insulin signaling is obviously crucial for understanding the control mechanisms of the system. As shown in Fig 5, multiple signaling is needed for the maintenance of glucose homeostasis. Below, we will discuss three major controls: glucose signaling on glucose fluxes, insulin signaling on glucose fluxes, and glucose signaling on insulin secretion. These regulatory interactions are usually referred to as glucose effectiveness, insulin sensitivity, and β-cell sensitivity. Their measurement requires that the system be probed with some experimental test inputs in order to activate the feedback mechanisms and to interpret the effect of these manouvers on the measured plasma concentration of glucose and insulin with some model of the system. We will discuss how glucose effectiveness, insulin sensitivity, and β-cell sensitivity can be measured in the steady- and non–steady-state.

Glucose Effectiveness

This parameter measures the effect of glucose to stimulate glucose disappearance rate, Rd, and to inhibit endogenous glucose production, EGP. Ideally, it should be measured in the absence of insulin. However, this is difficult, and glucose effectiveness must be referred to a given insulin concentration: basal (instead of "zero") insulin concentration is the usual reference.[4,81,82] A good reason for choosing basal insulin glucose effectiveness is that this parameter has a direct clinical relevance in situations where insulin secretory ability is severely impaired, eg, NIDDM.[82]

Glucose effectiveness is defined as follows:

$$\text{Glucose Effectiveness} = \left.\frac{\delta[\text{Rd}(t) - \text{EGP}(t)]}{\delta \text{G}(t)}\right|_{\text{I}=\text{I}_b} \tag{54}$$

where I_b denotes basal insulin concentration.

Glucose effectiveness can be measured from *steady-state* plasma glucose and insulin concentration data obtained with the hyperglycemic clamp technique maintaining insulin at the basal level. By using somatostatin to suppress insulin secretion and replacing basal levels of glucagon and insulin via an exogenous infusion of the two hormones, it is possible to investigate the effect of increasing levels of glucose on glucose disappearance and production, while maintaining insulin at the basal level. Glucose effectiveness can be quantified as the slope of the dose-response relationship between the steady-state glucose level and the exogenous glucose infusion rate used to raise the glucose level. In fact, by applying the above definition of glucose effectiveness one has:

$$\begin{aligned}\text{Clamp Glucose Effectiveness} &= \frac{\Delta[\text{Rd} - \text{EGP}]}{\Delta \text{G}} \\ &= \frac{\text{U}}{\Delta \text{G}} = \text{S}_{\text{G(damp)}}(\text{mL} \cdot \text{kg}^{-1} \cdot \text{min}^{-1})\end{aligned} \tag{55}$$

where U is the exogenous glucose infusion rate compensating at steady-state for the increase in Rd and the decrease in EGP.

By infusing a glucose tracer during the clamp, it is possible to assess the relative contributions of glucose actions on Rd and EGP. Specifically, the component of glucose effectiveness measuring the effect of glucose on Rd can be quantified from the relationship linking Rd to glucose concentration. The relationship between Rd and G is in all likelihood a curve that begins at zero and saturates at some plateau. Thus, a Michaelis-Menten model is probably a good candidate to describe it. However, in the range of glucose concentrations above the basal glucose level that are experienced in everyday life, a straight line with a nonzero intercept is a good model to represent Rd versus G. $S_{Gd(clamp)}$ is the slope of this linear relationship:

$$\text{Rd} = \text{S}_{\text{Gd(clamp)}}\text{G} + \text{Rd}_0. \tag{56}$$

and thus

$$S_{Gd(clamp)} = \frac{\Delta Rd}{\Delta G} (mL \cdot kg^{-1} \cdot min^{-1}) \quad (57)$$

It is important to recognize that the linear model fails as glucose approaches zero and that the nonzero intercept Rd_0 has no physiological meaning, ie, it only has an operational role when it comes to predict Rd as a function of G. It is also of interest that the presence of the nonzero intercept accounts for the fact that Rd does not increase proportionally to G and that glucose clearance rate decreases as glucose increases:

$$PCR = Rd/G = S_{Gd(clamp}G + Rd_0/G \quad (58)$$

Glucose effectiveness can also be measured from *non–steady-state* plasma glucose and insulin concentration data obtained with a glucose perturbation test.

Optimal probe. The optimal protocol for measuring glucose effectiveness is to give a glucose perturbation to produce a transient excursion of glucose above basal levels, while experimentally maintaining insulin basal with a somatostatin, insulin, and glucagon infusion.[82] Under these circumstances, glucose is the only dynamic determinant of glucose decay, and glucose effectiveness can be calculated in a model-independent way as:

$$GE = \frac{D}{AUC[\Delta C(t)]} (mL \cdot min^{-1} kg^{-1}) \quad (59)$$

where D is the amount of exogenous glucose administered and AUC[ΔC] is the area under the curve (AUC) of the glucose concentration excursion above basal (ΔC).

Glucose effectiveness can also be estimated by particularizing the minimal model of glucose disappearance[4] to this experimental situation (the insulin action term vanishes). The model reduces to[82]:

$$\begin{aligned} \dot{Q}_1(t) &= -S_G Q_1(t) + S_G Q_{1b} + U_1(t) \quad Q_1(0) = Q_{1b} \\ C_1(t) &= \frac{Q_1(t)}{V_1} \end{aligned} \quad (60)$$

where Q_1 is glucose mass, with Q_{1b} denoting its pretest basal value; U_1 is the glucose infusion rate; V_1 is the distribution volume; C_1 is plasma glucose concentration; and $S_G(min^{-1})$ is glucose effectiveness measuring the ability of glucose per se, in the presence of basal insulin, to stimulate Rd and to suppress EGP. Both parameters S_G and V_1 can be estimated from the glucose data.

The model-independent glucose effectiveness (GE) can be directly compared with the minimal model estimate of glucose effectiveness by considering the product $S_G V_1$. Recent results in humans show that GE and $S_G V_1$ are virtually equivalent, when insulin is kept at basal levels, both during a gross perturbation like an IVGTT,[83] as well as during a more gentle perturbation like the one producing a prandial glucose concentration profile.[82]

GE and $S_G V_1$ measure a composite "EGP plus Rd" glucose effectiveness. However, if a tracer (eg, [6-^{3}H]glucose) is concomitantly infused with glucose and its concentration measured in plasma, it is possible to dissect glucose effectiveness into its EGP and Rd components. The model-independent estimate of Rd glucose effectiveness, GE_d, is[82]:

$$GE_d = \frac{\{AUC[\Delta u(t)] - PCR\, C_b\, AUC[\Delta(c(t)/C(t))]\}}{\{AUC[\Delta c(t)] - C_b\, AUC[\Delta(c(t)/C(t))]\}} \quad (61)$$

$$(mg \cdot kg^{-1} \cdot min^{-1})$$

where Δ denotes above basal, u is the tracer infusion rate, c is tracer glucose concentration, C is glucose concentration (suffix b denotes basal), and PCR is the basal plasma glucose clearance rate.

One can also use the tracer version of the minimal model (equation 60) to estimate the Rd component of S_G, S_{Gd}[82] (S_{Gd} was denoted S_G^* by Basu et al[82]). The model equations are:

$$\begin{aligned} \dot{q}_1(t) &= -\left[S_{Gd} + \frac{Rd_0}{Q_1(t)}\right] q_1(t) + u_1(t) \quad q_1(0) = q_{1b} \\ y_1(t) &= \frac{q_1(t)}{v_1} \end{aligned} \quad (62)$$

where q_1 is plasma tracer glucose mass, with q_{1b} denoting its pretest value obtained with a basal tracer infusion rate u_{1b}; v_1 is the tracer distribution volume; y_1 is plasma tracer glucose concentration; S_{Gd} is glucose effectiveness on Rd; and Rd_0 is the nonzero intercept of the Rd versus Q_1 characteristic describing the inhibitory effect of glucose on Rd. Parameters S_{Gd}, Rd_0, and v_1 are related by the pretest steady-state constraint:

$$\dot{q}_1(t) = -\left[S_{Gd} + \frac{Rd_0}{Q_{1b}}\right] q_{1b} + u_{1b} = 0 \quad (63)$$

Thus, for instance, one can estimate S_{Gd} and v_1 from the tracer data and subsequently calculate Rd_0 from the constraint.

Recent results in humans show that GE_d and $S_{Gd}v_1$ are virtually equivalent measures for the prandial-like perturbation[82] (data on a basal insulin-labeled IVGTT protocol are not available).

The knowledge of the composite "EGP plus Rd" glucose effectiveness, GE and S_G, and that of its Rd component, GE_d and S_{Gd}, allows the calculation of the EGP component, GE_l and S_{Gl}, from:

$$GE_l = GE - GE_d \quad (64)$$

$$S_{Gl} = S_G - S_{Gd} \quad (65)$$

IVGTT probe. It would be convenient if glucose effectiveness, S_G, could be estimated from a simpler experiment, ie, one that does not require the inhibition of endogenous insulin secretion by somatostatin, like a standard IVGTT. In fact, this is possible by using the so-called minimal model of glucose kinetics (Fig 23), which relates plasma glucose and insulin concentrations measured during an IVGTT (standard, or modi-

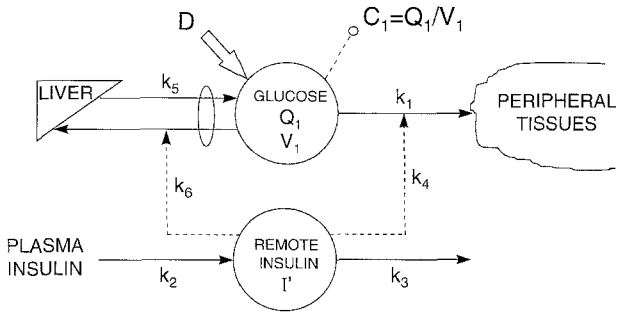

Fig 23. Single-compartment minimal model of glucose kinetics.

fied with a tolbutamide or insulin injection). The model, in its uniquely identifiable parameterization,[4,84] is described by:

$$\begin{aligned} \dot{Q}_1(t) &= -[p_1 + X(t)]Q_1(t) + p_1Q_{1b} \quad Q_1(0) = Q_{1b} + D \\ \dot{X}(t) &= -p_2X(t) + p_3[I(t) - I_b] \quad X(0) = 0 \\ C_1(t) &= Q_1(t)/V_1 \end{aligned} \tag{66}$$

where Q_1 is plasma glucose mass, with Q_{1b} denoting its basal value; I is plasma insulin concentration, with I_b denoting its basal value; D is the glucose dose; V_1 is the glucose distribution volume; X is insulin action (proportional to remote insulin I', $X = (k_4 + k_6)I'$); and p_i are parameters related to the k_i ($p_1 = k_1 + k_5$; $p_2 = k_3$; $p_3 = k_2(k_4 + k_6)$).

Parameters p_1, p_2, p_3, and V_1 can be estimated from the data and it can be shown[4] that glucose effectiveness, S_G, is given by:

$$S_G = p_1 = k_1 + k_5 \quad (\text{min}^{-1}) \tag{67}$$

As with the optimal protocol, if a tracer is added to the IVGTT bolus and its concentration measured in plasma, minimal modeling of insulin and tracer concentration data allow the estimation of the component of S_G, reflecting glucose effect on Rd.[5,84-87] The tracer minimal model (Fig 24), in its uniquely identifiable parameterization,[5,84] is given by:

$$\begin{aligned} \dot{q}_1(t) &= -[p_{1d} + x(t)]q_1(t) \quad q_1(0) = d \\ \dot{x}(t) &= -p_{2d}x(t) + p_{3d}[I(t) - I_b] \quad x(0) = 0 \\ y_1(t) &= \frac{q_1(t)}{v_1} \end{aligned} \tag{68}$$

where lowercase lettering and the suffix d are used to indicate the tracer version of the variables and parameters of equation 66 (in references 5 and 84 through 87, an asterisk (*) symbol was used to denote tracer variables and parameters); x is proportional to remote insulin i'($x = k_4i'$); and the p_{id} are parameters related to the k_i($p_{1d} = k_1$; $p_{2d} = k_3$; $p_{3d} = k_2k_4$).

Parameters p_{1d}, p_{2d}, p_{3d}, and v_1 can be estimated from the tracer data and it can be shown[5,84] that the Rd component of glucose effectiveness, S_{Gd}, is given by

$$S_{Gd} = p_1 = k_1 \quad (\text{min}^{-1}) \tag{69}$$

It is worth noting that, in this model, glucose effectiveness, S_{Gd}, coincides with the fractional glucose clearance at basal insulin, since $Rd_0 = 0$, ie, the inhibitory effect term Rd_0/Q of equation 62 is not accounted for.

The accuracy with which S_G and S_{Gd} are estimated from the two minimal models clearly depends on the ability of the two models to correctly describe dynamic insulin action on EGP and Rd (this is not requested in the optimal protocol, where insulin is kept basal). In addition, the IVGTT is a highly dynamic situation (in contrast with the smoother one provided by the optimal meal-like protocol) and a single compartment description of glucose kinetics may be inadequate. Evidence exists that a reliable description of glucose kinetics requires at least two compartments[1] and, in fact, to mitigate this error, minimal-model identification is performed by ignoring data for the first 8 to 10 minutes. Recently, several investigators have challenged both experimentally and theoretically some of the minimal-model assumptions.[5,6,84,86,88-97] It has been suggested[86,90,92,96,97] that both S_G and S_{Gd} suffer, albeit to a different extent, by monocompartmental undermodeling and that S_G also suffers by the minimal-model description of the control exerted by glucose and insulin on EGP.[5] In particular, for S_GV_1, a two/threefold overestimation, and a poor correlation was found when compared with the optimal protocol, ie, the basal insulin IVGTT, estimates of glucose effectiveness calculated either model-independently or with the minimal model.[83] Of particular interest are some results obtained using a two-compartment description of glucose kinetics: the physiologically absurd EGP profile derived by combining the two minimal models vanishes[6,62,63] and the overestimation of S_G experimentally observed by Quon et al[88] is explained.[90,92] Encouraged by these results, we have recently reexamined the domain of validity of S_G and S_{Gd} by using a two-compartment simulation model as a reference.[92,96,97] S_G reflects both the fast and the slow component of glucose disappearance and thus measures not only the ability of glucose to promote Rd and inhibit EGP, but also the exchange kinetics between the accessible and the slowly equilibrating glucose pool. S_G has thus a local domain of validity and overestimates glucose effectiveness. S_G has been also reported to be influenced by the insulin profile during the IVGTT[91]: in all likelihood, this undesidered dependence is also caused by monocompartmental undermodeling. S_{Gd} is not a good descriptor of glucose effectiveness on Rd unless an explicit description of the inhibitory effect of glucose on its own Rd is included in the model. However, S_{Gd} does not suffer by single-compartment undermodeling or by the insulin profile, and has a clear-cut physiologic interpretation, because it measures basal fractional glucose clearance rate.

A two-compartment (not so minimal!) model is the obvious next step to describe the IVGTT situation and alleviate the above problems. Unfortunately a two-compartment model is difficult to resolve without tracer data.[7,84] The model is shown in Fig 25. In addition to the accessible pool (compartment 1), a second nonaccessible pool is postulated. Insulin-independent glucose disposal takes place in the accessible pool, and is described as the sum of two components, one constant (eg,

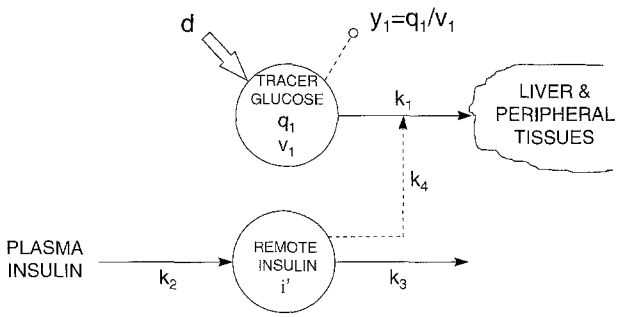

Fig 24. Tracer version of the model of Fig 23.

CNS) and the other proportional to glucose mass. This brings a time-varying rate constant describing the irreversible loss from the accessible pool:

$$k_{01}(t) = k_p + \frac{Rd_0}{Q_1(t)} \tag{70}$$

where Q_1 is the glucose mass, Rd_0 is the constant component of glucose disposal (assumed known and equal to 1 $mg \cdot kg^{-1}$ min^{-1}), and k_p accounts for the proportional-to-mass term.

Insulin-dependent glucose disposal occurs in the slowly exchanging pool and is described by allowing a parametric control of remote insulin on parameter k_{02}.

The physiologically based constraint used by Cobelli et al[1] to guarantee a priori identifiability has been retained, ie, it is assumed that in the basal state insulin-independent glucose disposal is three times insulin-dependent glucose disposal. This yields the following relation among the model parameters:

$$k_p + \frac{Rd_0}{Q_b} = \frac{3k_{21}k_{02}}{k_{02} + k_{12}} \tag{71}$$

This additional relation ensures a priori unique identifiability of the model:

$$\begin{aligned} \dot{q}_1(t) &= -[k_{01}(t) + k_{21}]q_1(t) + k_{12}q_2(t) \quad q_1(0) = d \\ \dot{q}_2(t) &= k_{21}q_1(t) - [k_{02} + x(t) + k_{12}]q_2(t) \quad q_2(0) = 0 \\ \dot{x}(t) &= -p_{2d}x(t) + p_{3d}[I(t) - I_b] \\ y_1(t) &= q_1(t)/v_1 \end{aligned} \tag{72}$$

where, like in the single-compartment model, one has $x = k_c i'$, $p_{2d} = k_b$, and $p_{3d} = k_a k_c$.

From the uniquely identifiable parameters, v_1, k_{21}, k_{12}, k_{02}, p_{2d}, and p_{3d}, glucose effectiveness and plasma glucose clearance rate can be derived. Glucose effectiveness, S^2_{Gd} (apex 2 denotes "two-compartment model"), is:

$$S^2_{Gd} = \left(k_p + \frac{k_{21}k_{02}}{k_{02} + k_{12}}\right) \quad (min^{-1}) \tag{72}$$

Plasma glucose clearance rate at basal insulin, PCR, is:

$$PCR = v_1\left(k_p + \frac{Rd_0}{Q_{1b}} + \frac{k_{21}k_{02}}{k_{02} + k_{12}}\right) \quad (mL \cdot min^{-1}kg^{-1}) \tag{74}$$

Note that, in contrast to the single-compartment minimal model, where glucose effectiveness and fractional clearance rate coincide, this is no longer true with the two-compartment model: S^2_{Gd} and PCR come out different due to the presence in the model of the inhibitory effect term $Rd_0/Q_1(t)$.

It is of interest to compare the single-compartment S_{Gd} with S^2_{Gd} and PCR. In normal humans,[7,84] S_{Gd} correlates rather weakly with both S^2_{Gd} and PCR. However, if PCR is divided by the total distribution volume available in each subject $[V_T = v_1(1 + k_{21}/k_{12} + k_{02})]$, one has that the regression line between PCR/V_T and S_{Gd} is not different from the identity line, confirming the fractional clearance nature of the single-compartment index.

Meal-like probe. The IVGTT is a highly dynamic probe that requires a rich model for its interpretation. However, without the addition of a tracer, it is difficult to resolve from the data a two-compartment model. On the other hand, the single-compartment model is affected by undermodeling. To overcome these limitations, a less dynamic probe should in principle help, because the degree of approximation of the single-compartment representation also depends on the input signal. If the glucose infusion rate changes rapidly, like during the IVGTT, the single-compartment model has difficulties in correctly interpreting the rapid changes in glucose concentration. In contrast, when glucose concentration changes slowly, like in a meal-like protocol, as a result of a more gentle glucose infusion, the monocompartmental model is less inaccurate. Recently, a meal-like protocol, ie, an experimental protocol in which plasma glucose and (with endogenous insulin secretion inhibited by a somatostatin, insulin and glucagon infusion) insulin concentration profiles mimick those typically observed during a meal, has been used in conjunction with the single-compartment minimal model.[98,99]

The model is described by equation 66 with a glucose infusion term U_I added to the glucose equation [with initial condition $Q_1(0) = Q_{1b}$]. From the model, one can estimate S_G and V_1. Our results[99] show that $S_G V_1$ is virtually equivalent to glucose effectiveness estimated from the optimal protocol,[82] ie, with basal insulin and prandial glucose concentration, either

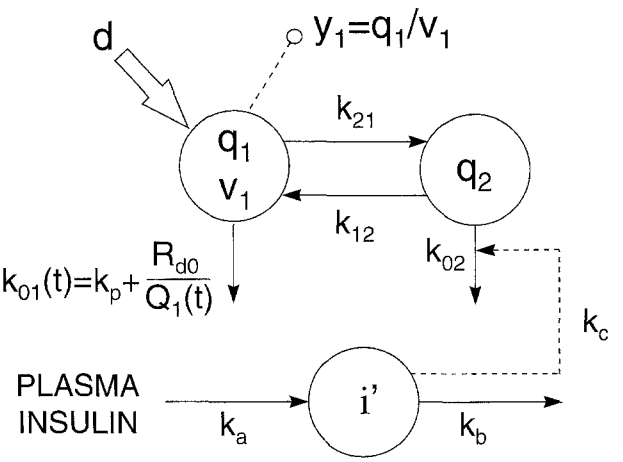

Fig 25. Two-compartment minimal model of tracer glucose kinetics.

model-independently (equation 59) or with the minimal model (equation 60).

If a tracer is added to the protocol, the model described by equation 68 with a tracer infusion term u_1 added to the glucose equation [with initial condition $q_1(0) = q_{1b}$] can be used to estimate S_{Gd} and v_1. Again $S_{Gd}v_1$ is virtually identically[99] to the Rd component of glucose effectiveness estimated during the tracer optimal protocol,[82] ie, with equations 61 and 62. Of note is also that the inconsistency between S_G and S_{Gd} that was observed with the IVGTT,[5,86,96] ie, S_G is three times higher than S_{Gd}, in contrast to the results from clamp studies, where the factor is 1.5, vanishes with this more gentle protocol.

Insulin Sensitivity

This parameter measures the effect of insulin to enhance the glucose per se stimulation of Rd and inhibition of EGP and can be formally defined as the ability of insulin to increase glucose effectiveness at steady-state:

$$\text{Insulin Sensitivity} = \left.\frac{\delta\text{Glucose Effectiveness(t)}}{\delta I(t)}\right|_{ss} \quad (75)$$

where ss denotes steady-state.

Insulin sensitivity can be measured from *steady-state* plasma glucose and insulin concentration data by using the euglycemic-hyperinsulinemic clamp. By this method, insulinemia is elevated by a constant insulin infusion and glucose is maintained at the basal level by a variable glucose infusion. Under these conditions, the glucose infusion needed to maintain euglycemia is a measure of the ability of insulin to suppress EGP and stimulate Rd. In fact, by applying the above definition of insulin sensitivity to the glucose clamp, we have:

$$\text{Clamp Insulin Sensitivity} = \frac{\Delta[R_d - \Delta EGP]}{G\Delta I} = \frac{U}{G\Delta I} = S_{I(clamp)}\,(mL \cdot min^{-1} \cdot kg \text{ per } \mu U \cdot mL^{-1}) \quad (76)$$

The effect of insulin on Rd only can be differentiated by infusing a glucose tracer during the clamp. This component of overall insulin sensitivity is termed as $S_{Id(clamp)}$. $S_{Id(clamp)}$ is the steady-state ratio of the increment in glucose uptake to the increment in plasma insulin concentration, normalized to the ambient glucose concentration at which the clamp is performed:

$$S_{Id(clamp)} = \frac{\Delta R_d}{G\Delta I}\,(mL \cdot min^{-1} \cdot kg \text{ per } \mu U \cdot mL^{-1}) \quad (77)$$

Insulin sensitivity can also be measured from *non–steady-state* plasma glucose and insulin concentration data by employing the IVGTT or a meal-like probe.

IVGTT probe. The IVGTT (either in its standard form or modified with a tolbutamide or insulin injection) interpreted with the minimal model (equation 66) has been widely used since its proposition in 1979.[4] The model explains the glucose and insulin concentration data by involving two concepts; the first one is the effects of glucose at basal insulin discussed above, and the second one is insulin sensitivity, ie, the effect of the above-basal dynamic component of insulin on Rd and EGP. It can be shown[4,84] that insulin sensitivity, S_I, is given by:

$$S_L = \frac{p_3}{p_2} = \frac{k_2(k_4 + k_6)}{k_3} \quad (min^{-1} \text{ per } \mu U \cdot mL^{-1}) \quad (78)$$

S_I measures the ability of insulin to enhance the glucose stimulation of Rd and inhibition of EGP.

The estimation of the Rd component of S_I is possible if a tracer is employed. In this case, from the tracer minimal model (equation 68), one has[5,84]:

$$S_{Id} = \frac{p_{3d}}{p_{2d}} = \frac{k_2k_4}{k_3} \quad (min^{-1} \text{ per } \mu U \cdot mL^{-1}) \quad (79)$$

Which is the domain of validity of S_I and S_{Id} in light of the critical reexamination of the domain of validity of S_G and S_{Gd}? Our theoretical and simulation results[90,92,96,97] show that the overestimation of S_G causes a marked underestimation of S_I, but S_I maintains a high correlation with that provided by a reference two-compartment model. In contrast, S_{Id} is only slightly underestimated. Finally, it should remembered that the accuracy of S_I, but not S_{Id}, also depends on the reliability of the description of glucose and insulin control on EGP embodied in the model (equation 66) and recent studies[6,62,63] question the underlying assumptions.

As discussed earlier, the tracer data allow the resolution of a two-compartment minimal model (equation 72). Insulin sensitivity can be calculated as[7]:

$$S^2_{Id} = v_1 \frac{p_{3d}k_{21}k_{12}}{p_{2d}(k_{02} + k_{12})^2}\,(mL \cdot min^{-1} \cdot kg \text{ per } \mu U \cdot mL^{-1}) \quad (80)$$

The single-compartment index, S_{Id}, and the two-compartment one, S^2_{Id}, correlate very strongly.[7,84] Of note is that when they are brought to the same units by multiplying S_{Id} by the volume of the single-compartment model v_1, the regression line between $S_{Id}v_1$ and S^2_{Id} is not different from the identity line.

Meal-like probe. The single-compartment minimal models of equations 66 and 68 (with the modifications discussed in Glucose Effectiveness) can be used to estimate S_I and S_{Id}, respectively.[99] Like with glucose effectiveness, the inconsistency between S_I and S_{Id} observed with the IVGTT,[5,86,96] ie, S_I lower than S_{Id} contrary to theoretical expectation, vanishes with this protocol.

β-Cell Sensitivity

This parameter measures the effect of glucose to stimulate β-cell insulin secretion. Usually a glucose perturbation is given, and from the glucose and C-peptide concentrations measured in plasma, one estimates β-cell sensitivity. A few quantitative approaches are available, but they have not been critically compared. One approach is based on relating plasma glucose and insulin secretion rate reconstructed by the deconvolution from C-peptide plasma concentration measured during a graded glucose infusion protocol.[100] Another steady-state ap-

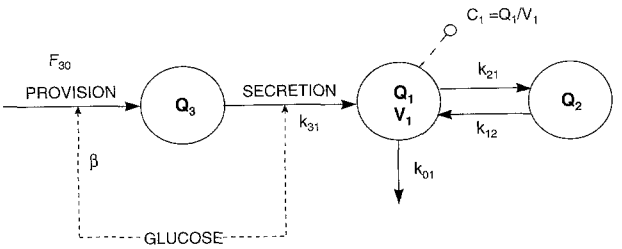

Fig 26. C-peptide minimal model.

proach uses an oscillatory glucose infusion input and spectral analysis of the glucose and C-peptide plasma concentrations.[101] Another approach is based on the interpretation of the non–steady-state glucose and C-peptide plasma concentrations measured during an IVGTT with the C-peptide minimal model.[102] This last approach aims to characterize parametrically insulin secretion by using an approach similar to what we have done for the glucose system. The model (Fig 26) explains the glucose and C-peptide (secreted equimolarly with insulin, but not extracted by the liver) concentration data by postulating a specific functional relationship between insulin secretion and glucose concentration, and using a two-compartment model to describe C-peptide kinetics. The model equations (in terms of deviations from basal of C-peptide masses and insulin secretion) are:

$$\begin{aligned}
\dot{Q}_1(t) &= -(k_{01} + k_{21})Q_1(t) + k_{12}Q_2(t) + k_{31}Q_3(t) \quad Q_1(0) = 0 \\
\dot{Q}_2(t) &= -k_{12}Q_2(t) + k_{21}Q_1(t) \quad Q_2(0) = 0 \\
\dot{Q}_3(t) &= -k_{31}Q_3(t) + F_{30}(t) \quad Q_3(0) = Q_{30} \\
\dot{F}_{30}(t) &= -\alpha[F_{30}(t) - \beta(G(t) - h)] \quad F_{30}(0) = 0 \\
C_1(t) &= \frac{Q_1(t)}{V_1}
\end{aligned} \tag{81}$$

where Q_1 and Q_2 are C-peptide masses in the accessible and peripheral compartments, respectively; Q_3 is C-peptide mass in β-cells; F_{30} is provision of new insulin to β-cells; k_{ij}, α, and β are rate parameters; h is a threshold level; V_1 is the volume of the accessible compartment; and C_1 is the measured C-peptide concentration.

Once the parameters of C-peptide kinetics k_{21}, k_{01}, k_{12}, and V_1 are fixed (via a separate experiment or by using available standard values[74]), the parameters k_{31}, α, β, h, and Q_{30} are uniquely identifiable and can be used to estimate, in addition to insulin secretion rate given by $k_{31}Q_3(t)$, indices of β-cell sensitivity to glucose.

The first-phase sensitivity to glucose, ϕ_1, is:

$$\phi_1 = \frac{Q_{30}}{\Delta G} \text{ (unitless)} \tag{82}$$

where ΔG is maximum increment of plasma glucose concentration following the injection.

The second-phase sensitivity to glucose, ϕ_2, is:

$$\phi_2 = \beta \text{ (min}^{-1}\text{)} \tag{83}$$

A sensitivity index can also be defined for basal insulin secretion, ϕ_b, as:

$$\phi_b = \frac{k_{01}C_{1b}}{G_b} \text{ (min}^{-1}\text{)} \tag{84}$$

where the suffix b denotes the basal value.

This parametric portrait of β-cell function can be drawn both from a standard, as well as from an insulin-modified IVGTT.[103] Of note is that this last test also allows the estimation of hepatic insulin extraction by employing a similar modeling rationale to the insulin data.[104] The secretory portion of the C-peptide model of equation 81 is used to describe posthepatic insulin delivery in conjunction with a linear single-compartment model of insulin kinetics. Since the posthepatic secretory parameters of the model implicitely take into account hepatic insulin secretion by relating them to those of the C-peptide model, one should be able to infer quantitatively on insulin extraction by the liver. In fact, from the parameters of the insulin minimal model, three indices can be estimated, ϕ_1^p, ϕ_2^p, and ϕ_b^p (p denotes posthepatic), which quantify the sensitivity to glucose of posthepatic insulin secretion. By comparing these indices with ϕ_1, ϕ_2, and ϕ_b of equations 82 through 84, it is possible to evaluate the fraction of secreted insulin that is extracted by the liver during first phase, HE_1, second phase, HE_2, and basal, HE_b, insulin secretion as:

$$HE_1 = 1 - \phi_1^p V_I/\phi_1 V_c \tag{85}$$

$$HE_2 = 1 - \phi_2^p V_I/\phi_2 V_c \tag{86}$$

$$HE_b = 1 - \phi_b^p V_I/\phi_b V_c \tag{87}$$

where $V_c = V_1$ (see equation 81) and V_I denotes the insulin distribution volume. Recent results[104] show that, on average, insulin extraction indices are approximately the same (≃60%) in the basal state and during the first- and second-phase responses to the glucose stimulus.

CONCLUSION

The measurement of nonaccessible system parameters requires a model of the system and a suitably designed tracer experiment. Both of these components are necessary for a quantitative understanding of the system according to the "garbage in–garbage out" paradigm (Fig 27). While the neces-

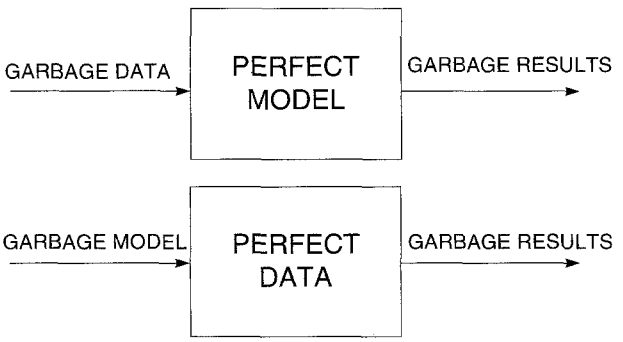

Fig 27. "Garbage in–garbage out" paradigm.

sity of good quality data is normally considered an obvious prerequisite, that of a good quality interpretative model is often not fully appreciated. In this report, we have discussed the fundamentals of the model of system methodology focusing on compartmental and input-output modeling. The glucose system has been our proof of the pudding, and models to measure glucose fluxes, insulin fluxes, and glucose-insulin signaling have been discussed.

REFERENCES

1. Cobelli C, Toffolo G, Ferrannini E: A model of glucose kinetics and their control by insulin. Compartmental and noncompartmental approaches. Math Biosci 72:291-315, 1984
2. Ferrannini E, Smith DJ, Cobelli C, et al: Effect of insulin on the distribution and disposition of glucose in man. J Clin Invest 76:357-364, 1985
3. Taylor R, Magnusson I, Rothman DL, et al: Direct assessment of liver glycogen storage by ^{13}C nuclear magnetic resonance spectroscopy and regulation of glucose homeostasis after a mixed meal in normal subjects. J Clin Invest 97:126-132, 1996
4. Bergman RN, Ider YZ, Bowden CR, et al: Quantitative estimation of insulin sensitivity. Am J Physiol 236:E667-E677, 1979
5. Cobelli C, Pacini G, Toffolo G, et al: Estimation of insulin sensitivity and glucose clearance from minimal model: new insights from labelled IVGTT. Am J Physiol 250:E591-E598, 1986
6. Caumo A, Cobelli C: Hepatic glucose production during the labeled IVGTT: Estimation by deconvolution with a new minimal model. Am J Physiol 264:E829-E841, 1993
7. Vicini P, Caumo A, Cobelli C: The hot IVGTT two compartment minimal model: Indices of glucose effectiveness and insulin sensitivity. Am J Physiol 273:E1024-E1031, 1997
8. Saccomani MP, Cobelli C: Qualitative experiment design in physiological system identification. IEEE Control Systems Magazine 12:18-23, 1992
9. Saccomani MP, Cobelli C: A minimal input-output configuration for a priori identifiability of a compartmental model of leucine metabolism. IEEE Trans Biomed Eng 40:797-803, 1993
10. Sacca' L, Toffolo G, Cobelli C: The V-A and A-V modes in whole body and regional kinetics: Domain of validity from a physiological model. Am J Physiol 262:E597-E606, 1992
11. Cobelli C, Toffolo G, Foster D: Tracer-to-tracee ratio for analysis of stable isotope tracer data: Link with radioactive kinetic formalism. Am J Physiol 263:E968-E975, 1992
12. Carson ER, Cobelli C, Finkelstein L: The Mathematical Modelling of Metabolic and Endocrine Systems. New York, NY, Wiley, 1983
13. Jacquez JA: Compartmental Analysis in Biology and Medicine (ed 3). Ann Arbor, MI, BioMedware, 1996
14. Berman M, Grundy SM, Howard BV (eds): Lipoprotein Kinetics and Modeling. New York, NY, Academic, 1982
15. Cobelli C, Bergman RN (eds): Carbohydrate Metabolism. Chichester, UK, Wiley, 1981
16. Cramp DG (ed): Quantitative Approaches to Metabolism. Chichester, UK, Wiley, 1982
17. Gibaldi M, Perrier D: Pharmacokinetics (ed 2). New York, NY, Marcel Dekker, 1982
18. Rowland M, Tozer T: Clinical Pharmacokinetics: Concepts and Applications (ed 3). Baltimore, MD, Williams & Wilkins, 1995
19. Carson ER, Jones EA: The use of kinetic analysis and mathematical modeling in the quantitation of metabolic pathways in vivo: Application to hepatic anion metabolism. N Engl J Med 300:1016-1027, 1078-1086, 1979
20. Cobelli C: Modeling and identification of endocrine-metabolic systems. Theoretical aspects and their importance in practice. Math Biosci 72:263-289, 1984
21. Cobelli C, Bier DM, Ferrannini E: Modeling glucose metabolism in man: Theory and practice. Horm Metab Res 24:1-10, 1990 (suppl)
22. Foster DM, Boston RC: The use of computers in compartmental analysis: The SAAM and CONSAM programs, in Robertson J (ed): Compartmental Distribution of Radiotracers. Boca Raton, FL, CRC, 1983, pp 73-142
23. Barrett PHR, Bell BM, Cobelli C, et al: SAAM II: Simulation, analysis, and modeling software for tracer and pharmacokinetic studies. Metabolism 47:484-492, 1998
24. Rescigno A, Gurpide E: Estimation of average times of residence, recycles and interconversion of blood-borne compounds using tracer methods. J Clin Endocrinol Metab 36:263-276, 1973
25. DiStefano JJ III: Noncompartmental vs. compartmental analysis: Some bases for choice. Am J Physiol 243:R1-R6, 1982
26. Cobelli C, Toffolo G: Compartmental versus noncompartmental modeling for two accessible pool. Am J Physiol 247:R488-R496, 1984
27. Cobelli C, DiStefano JJ III: Parameter and structural identifiability concepts and ambiguities: A critical review and analysis. Am J Physiol 239:R7-R24, 1980
28. Godfrey KR, DiStefano JJ III: Identifiability of model parameters, in Walter E (ed): Identifiability of Parametric Models. Oxford, UK, Pergamon, 1987, pp. 1-20
29. Cobelli C, Lepschy A, Romanin Jacur G: Identifiability results on some constrained compartmental systems. Math Biosci 47:173-196, 1979
30. Norton JP: An investigation of the sources of non-uniqueness in deterministic identifiability. Math Biosci 60:89-108, 1982
31. DiStefano JJ III: Complete parameter bounds and quasiidentifiability conditions for a class of unidentifiable linear systems. Math Biosci 65:51-68, 1983
32. Pohjanpalo H: System identifiability based on the power series expansion of the solution. Math Biosci 41:21-34, 1978
33. D'Angio' L, Audoly S, Bellu G, et al: Structural identifiability of nonlinear systems: Algorithms based on differential ideals, in Blanke M, Söderstrom T (eds): Proceedings of the 10th IFAC Symposium on System Identification, vol 3. Copenhagen, Denmark, Danish Automation Society, 1994, pp 13-18
34. Ljung L, Glad T: On global identifiability for arbitrary model parameterizations. Automatica 30:265-276, 1994
35. Audoly S, D'Angio' L, Saccomani MP, et al: Global identifiability of linear compartmental models. A computer algebra algorithm. IEEE Trans Biomed Eng 45:36-47, 1998
36. Cobelli C, Toffolo G: Theoretical aspects and practical strategies for the identification of unidentifiable compartmental systems, in Walter E (ed): Identifiability of Parametric Models. Oxford, UK, Pergamon, 1987, pp 85-91
37. Landaw EM, DiStefano JJ III: Multiexponential, multicompartmental, and noncompartmental modeling II. Data analysis and statistical considerations. Am J Physiol 246:R665-R677, 1984
38. D'Argenio DZ: Optimal sampling times for pharmacokinetic experiments. J Pharmacokinet Biopharm 9:739-757, 1981
39. DiStefano JJ III: Optimized blood sampling protocols and sequential design of kinetic experiments. Am J Physiol 9:R259-R265, 1981
40. Cobelli C, Ruggeri A, DiStefano JJ III, et al: Optimal design of multioutput sampling schedules: Software and applications to endocrine-metabolic and pharmacokinetic models. IEEE Trans Biomed Eng 32:249-256, 1995
41. DiStefano JJ III, Jang M, Malone TK, et al: Comprehensive kinetics of triiodothyronine (T_3) production, distribution and metabo-

lism in blood and tissue pools of the rat using optimized blood sampling protocols. Endocrinology 110:198-213, 1982

42. Cobelli C, Ruggeri A: Optimal design of sampling schedules for studying glucose kinetics with tracers. Am J Physiol 257:E444-E450, 1989

43. Cobelli C, Ruggeri A: A reduced sampling schedule for estimating the parameters of the glucose minimal model from a labelled IVGTT. IEEE Trans Biomed Eng 38:1023-1029, 1991

44. Cobelli C, Thomaseth K: The minimal model of glucose disappearance: Optimal input studies. Math Biosci 83:127-155, 1987

45. Cobelli C, Thomaseth K: On optimality of the impulse input for linear system identification. Math Biosci 89:127-133, 1988

46. Cobelli C, Thomaseth K: Optimal equidose inputs and role of measurement error for estimating the parameters of a compartmental model of glucose kinetics from continuous- and discrete-time optimal samples. Math Biosci 89:135-147, 1988

47. De Nicolao G, Sparacino G, Cobelli C: Nonparametric input estimation in physiological systems: Problem, methods, case studies. Automatica 33:851-870, 1997

48. Cobelli C, Carson ER, Finkelstein L: Validation of simple and complex models in physiology and medicine. Am J Physiol 246:R259-R266, 1984

49. Bonadonna R, Saccomani MP, Cobelli C: In vivo glucose transport in human skeletal muscle: tools, problems and perspectives. Bailliere Clin Endocrinol Metab 7:929-960, 1993

50. Saccomani MP, Bonadonna R, Bier DM, et al: A model to measure insulin effects on glucose transport and phosphorylation in muscle: A three-tracer study. Am J Physiol 33:E170-E185, 1996

51. Bonadonna RC, Del Prato S, Bonora E, et al: Roles of glucose transport and glucose phosphorylation in muscle insulin resistance of NIDDM. Diabetes 45:915-925, 1996

52. Kelley DE, Mintun MA, Watkins SC, et al: The effect of non–insulin-dependent diabetes mellitus and obesity on glucose transport and phosphorylation in skeletal muscle. J Clin Invest 97:2705-2713, 1996

53. Sokoloff L, Reivich M, Kennedy C, et al: The [^{14}C]deoxyglucose method for the measurement of local celebral glucose utilization: Theory, procedure and normal values in the conscious and anesthetized albino rat. J Neurochem 28:897-916, 1977

54. Phelps ME, Huang SC, Hoffman EJ, et al: Tomographic measurement of local cerebral glucose metabolic rate in humans with (F-18) fluoro-2-deoxy-D-glucose: Validation of method. Ann Neurol 6:371-388, 1979

55. Steele R, Wall J, De Bodo R, et al: Measurement of the size and turnover rate of the body glucose pool by the isotope dilution method. Am J Physiol 187:15-24, 1956

56. Finegood DT, Bergman RN, Vranic M: Estimation of endogenous glucose production during hyperinsulinemic-euglycemic glucose clamps: Comparison of unlabeled and labeled exogenous infusates. Diabetes 36:914-924, 1987

57. Butler PC, Caumo A, Zerman A, et al: Methods for the assessment of the rate of onset and offset of insulin action during nonsteady state in humans. Am J Physiol 264:E548-E560, 1993

58. Yki-Jarvinen H, Young AA, Lamkin C, et al: Kinetics of glucose disposal in whole body and across the forearm in man. J Clin Invest 79:1713-1719, 1987

59. Cobelli C, Mari A, Ferrannini E: Non-steady state: Error analysis of Steele's model and developments for glucose kinetics. Am J Physiol 252:E679-E689, 1987

60. Radziuk J, Norwich KH, Vranic M: Experimental validation of measurements of glucose turnover in non-steady state. Am J Physiol 234:E84-E93, 1978

61. Caumo A, Gelisio A, Rizza RA, et al: Models to measure hepatic glucose release in nonsteady state: A general validation strategy based on dual-tracer administration and convolution, in Patterson BW (ed): Proceedings of the 2nd IFAC Symposium on Modeling and Control in Biomedical Systems. Galveston, TX, Omnipress, 1994, pp 306-307

62. Vicini P, Zachwieja JJ, Yarasheski K, et al: Hepatic glucose release during the IVGTT: Concordance between two-compartment minimal model and specific activity clamp estimates. Diabetes 44: 156A, 1995 (suppl 1, abstr)

63. Vicini P, Sparacino G, Caumo A, et al: Estimation of endogenous glucose production after a glucose perturbation by nonparametric stochastic deconvolution. Comput Meth Progr Biomed 52:147-156, 1997

64. Jaquez JA: Theory of production rate calculations in steady and non-steady states and its application to glucose metabolism. Am J Physiol 262:E779-E790, 1992

65. Norwich KN: Molecular Dynamics. The Kinetics of Tracers in the Intact Organism. Oxford, UK, Pergamon, 1977

66. Caumo A, Homan M, Katz H, et al: Glucose turnover in presence of changing glucose concentrations: Error analysis for glucose disappearance. Am J Physiol 269:E557-E567, 1995

67. Polonsky KS, Licinio-Paizao J, Given BD, et al: Use of biosynthetic human C-peptide in the measurement of insulin secretion rates in normal volunteers and type I diabetic patients. J Clin Invest 77:98-105, 1986

68. Ferrannini E, Cobelli C: The kinetics of insulin in man. II. Role of the liver. Diabetes Metab Rev 3:365-397, 1987

69. Licinio-Paixao J, Polonsky KS, Given BD, et al: Ingestion of a mixed meal does not affect the metabolic clearance of biosynthetic human C-peptide. J Clin Endocrinol Metab 63:401-406, 1986

70. Shapiro ET, Tillil H, Rubenstein AH, et al: Peripheral insulin parallels changes in insulin secretion more closely than C-peptide after bolus intravenous glucose administration. J Clin Endocrinol Metab 67:1094-1099, 1988

71. Sparacino G, Cobelli C: Impulse response model in reconstruction of insulin secretion by deconvolution: Role of input design in the identification experiment. Ann Biomed Eng 25:398-416, 1997

72. Eaton RP, Allen RC, Schade DS, et al: Prehepatic insulin production in man: Kinetic analysis using peripheral connecting peptide behavior. J Clin Endocrinol Metab 51:520-528, 1980

73. Sparacino G, Cobelli C: A stochastic deconvolution method to reconstruct insulin secretion rate after a glucose stimulus. IEEE Trans Biomed Eng 43:512-529, 1996

74. Van Cauter E, Mestrez F, Sturis J, et al: Estimation of insulin secretion rates from C-peptide levels: Comparison of individual and standard parameters for C-peptide clearance. Diabetes 41:368-377, 1992

75. Polonsky KS, Given BD, Hirsch L, et al: Quantitative study of insulin secretion and clearance in normal and obese subjects. J Clin Invest 81:435-441, 1988

76. Polonsky KS, Given BD, Van Cauter E: Twenty-four-profiles and pulsatile patterns of insulin secretion in normal and obese subjects. J Clin Invest 81:442-448, 1988

77. Shapiro ET, Tillil H, Miller MA, et al: Insulin secretion and clearance. Comparison after oral and intravenous glucose. Diabetes 36:1365-1371, 1987

78. Tillil H, Shapiro ET, Miller MA, et al: Dose-dependent effects of oral and intravenous glucose on insulin secretion and clearance in normal humans. Am J Physiol 254:E349-E357, 1988

79. Ferrannini E, Cobelli C: The kinetics of insulin in man. I. General aspects. Diabetes Metab Rev 3:335-363, 1987

80. Morishima T, Pye S, Bradshaw L, et al: Posthepatic rate of appearance of insulin: Measurement and validation in the nonsteady state. Am J Physiol 263:E772-E779, 1992

81. Best JD, Khan SE, Ader M, et al: Role of glucose effectiveness in the determination of glucose tolerance. Diabetes Care 19:1018-1030, 1996

82. Basu A, Caumo A, Bettini F, et al: Impaired basal glucose

effectiveness in NIDDM. Contribution of defects in glucose disappearance and production measured using an optimized minimal model independent protocol. Diabetes 46:421-432, 1997

83. Bettini F, Caumo A, Quon MJ, et al: A model-independent measure of glucose effectiveness: Equivalence with minimal model estimate of S_G in absence of an insulin response but overestimation of S_G in the presence of an insulin response. Diabetes 46:245A, 1997 (suppl 1, abstr)

84. Cobelli C, Vicini P, Toffolo G, et al: The hot IVGTT minimal models: Simultaneous assessment of disposal indices and endogenous glucose production, in Bergman RN, Lovejoy JC (eds): The Minimal Model Approach and Determination of Glucose Tolerance. Baton Rouge, LA, Louisiana State University, 1997, pp 202-239

85. Avogaro A, Bristow JD, Bier DM, et al: Stable-label intravenous glucose tolerance test minimal model. Diabetes 38:1048-1055, 1989

86. Caumo A, Giacca A, Morgese M, et al: Minimal models of glucose disappearance: lessons from the labelled IVGTT. Diabetic Med 8:822-832, 1991

87. Avogaro A, Vicini P, Valerio A, et al: The hot but not the cold minimal model allows precise assessment of insulin sensitivity in NIDDM subjects. Am J Physiol 270:E532-E540, 1996

88. Quon MJ, Cochran C, Taylor SI, et al: Non-insulin-mediated glucose disappearance in subjects with IDDM. Discordance between experimental results and minimal model analysis. Diabetes 43:890-896, 1994

89. Saad MF, Anderson RL, Laws A, et al: A comparison between the minimal model and the glucose clamp in the assessment of insulin sensitivity across the spectrum of glucose tolerance. Diabetes 43:1114-1121, 1994

90. Caumo A, Vicini P, Cobelli C: Is the minimal model too minimal? Diabetologia 39:997-1000, 1996

91. Finegood DT, Tzur D: Reduced glucose effectiveness associated with reduced insulin release: an artifact of the minimal-model method. Am J Physiol 271:E485-E495, 1996

92. Cobelli C, Vicini P, Caumo A: If the minimal model is too minimal, who suffers more: S_G or S_I? Diabetologia 40:362-363, 1997

93. Saad MF, Steil GM, Kades WW, et al: Differences between the tolbutamide-boosted and the insulin-modified minimal model protocols. Diabetes 46:1167-1171, 1997

94. Ader M, Ni T-C, Bergman RN: Glucose effectiveness assessed under dynamic and steady state conditions. Comparability of uptake vs production component. J Clin Invest 99:1187-1199, 1997

95. Ni T-C, Ader M, Bergman RN: Reassessment of glucose effectiveness and insulin sensitivity from minimal model analysis: A theoretical evaluation of the single-compartment glucose distribution assumption. Diabetes 46:1813-1821, 1997

96. Caumo A, Vicini P, Zachwieja JJ, et al: Undermodeling affects minimal model indices: Insights from a two-compartment model. Am J Physiol (in press)

97. Vicini P, Caumo A, Cobelli C: Glucose effectiveness and insulin sensitivity from the minimal models: Consequences of undermodeling assessed by Monte Carlo simulation. IEEE Trans Biomed Eng (in press)

98. Alzaid AA, Dinneen SF, Turk DJ, et al: Assessment of insulin action and glucose effectiveness in diabetic and nondiabetic humans. J Clin Invest 94:2341-2348, 1994

99. Bettini F, Caumo A, Cobelli C: Minimal models in the meal-like protocols: Simulation studies to assess precision and physiological plausibility of parameter estimates, in Roberge FA, Kearney RE (eds): Proceedings of the 17th IEEE-EMBS. Montreal, Canada, IEEE, 1995, pp 1361-1362

100. Byrne MM, Sturis J, Polonsky KS: Insulin secretion and clearance during low-dose graded glucose infusion. Am J Physiol 268:E21-E27, 1995

101. Sturis J, Van Cauter E, Blackman JD, et al: Entrainment of pulsatile insulin secretion by oscillatory glucose infusion. J Clin Invest 87:439-445, 1991

102. Toffolo G, De Grandi F, Cobelli C: Estimation of β-cell sensitivity from intravenous glucose tolerance test C-peptide data. Knowledge of the kinetics avoids errors in modeling the secretion. Diabetes 44:845-854, 1995

103. Toffolo G, Cefalu WT, Cobelli C: Insulin modified IVGTT also allows functional assessment of beta-cell secretion by a new minimal model of C-peptide data. Diabetologia 38:A30, 1995 (suppl 1, abstr)

104. Toffolo G, Arduini A, De Zanche N, et al: A minimal model of insulin during insulin modified IVGTT: Assessment of hepatic insulin extraction, in Linkens DA, Carson E (eds): Proceedings of the 3rd IFAC Symposium on Modeling and Control in Biomedical Systems. 1997, pp 91-95